

**AD-A273 787**



②

**Third Quarter  
1993**

**S DTIC  
ELECTE  
DEC 15 1993  
A**

# **AFRRI Reports**

**93-30328**



3808

**93 12 14 063**

**REPORT DOCUMENTATION PAGE**Form Approved  
OMB No. 0704-0188

Public reporting burden for this collection of information is estimated to average 1 hour per response, including the time for reviewing instructions, searching existing data sources, gathering and maintaining the data needed, and completing and reviewing the collection of information. Send comments regarding this burden estimate or any other aspect of the collection of information, including suggestions for reducing this burden, to Washington Headquarters Service, Directorate for Information Operations and Reports, 1215 Jefferson Davis Highway, Suite 1204, Arlington, VA 22202-4302, and to the Office of Management and Budget, Paperwork Reduction Project (0704-0188), Washington, DC 20503

1. AGENCY USE ONLY (Leave blank)		2. REPORT DATE October 1993	3. REPORT TYPE AND DATES COVERED Reprints	
4. TITLE AND SUBTITLE AFRRI Reports, Third Quarter 1993			5. FUNDING NUMBERS PE: NWED QAXM	
6. AUTHOR(S)				
7. PERFORMING ORGANIZATION NAME(S) AND ADDRESS(ES) Armed Forces Radiobiology Research Institute 8901 Wisconsin Avenue Bethesda, MD 20889-5603			8. PERFORMING ORGANIZATION REPORT NUMBER SR93-20 - SR93-22	
9. SPONSORING/MONITORING AGENCY NAME(S) AND ADDRESS(ES) Uniformed Services University of the Health Sciences 4301 Jones Bridge Road Bethesda, MD 20814-4799			10. SPONSORING/MONITORING AGENCY REPORT NUMBER	
11. SUPPLEMENTARY NOTES				
12a. DISTRIBUTION/AVAILABILITY STATEMENT Approved for public release; distribution unlimited.			12b. DISTRIBUTION CODE	
13. ABSTRACT (Maximum 200 words) This volume contains AFRRI Scientific Reports SR93-20 through SR93-22 for July-September 1993.				
14. SUBJECT TERMS			15. NUMBER OF PAGES 38	
			16. PRICE CODE	
17. SECURITY CLASSIFICATION OF REPORT UNCLASSIFIED	18. SECURITY CLASSIFICATION OF THIS PAGE UNCLASSIFIED	19. SECURITY CLASSIFICATION OF ABSTRACT UNCLASSIFIED	20. LIMITATION OF ABSTRACT UL	

# CONTENTS

## Scientific Reports

**SR93-20:** Colden-Stanfield M, Ratcliffe D, Cramer EB, Gallin EK. Characterization of influenza virus-induced leukocyte adherence to human umbilical vein endothelial cell monolayers.

**SR93-21:** May LT, Neta R, Moldawer LL, Kenney JS, Patel K, Sehgal PB. Antibodies chaperone circulating IL-6: Paradoxical effects of anti-IL-6 "neutralizing" antibodies in vivo.

**SR93-22:** Patchen ML, Brook I, Elliott TB, Jackson WE. Adverse effects of pefloxacin in irradiated C3H/HeN mice: Correction with glucan therapy.

Accession For	
NTIS CRA&I	<input checked="" type="checkbox"/>
DTIC TAB	<input type="checkbox"/>
Unannounced	<input type="checkbox"/>
Justification .....	
By .....	
Distribution/	
Availability Codes	
Dist	Avail and/or Special
A-1	

**DTIC QUALITY INSPECTED 3**

# Characterization of Influenza Virus-Induced Leukocyte Adherence to Human Umbilical Vein Endothelial Cell Monolayers<sup>1</sup>

Margaret Colden-Stanfield,<sup>2\*</sup> Don Ratcliffe,<sup>†</sup> Eva B. Cramer,<sup>†</sup> and Elaine K. Gallin<sup>\*</sup>

<sup>\*</sup>Department of Physiology, Armed Forces Radiobiology Research Institute, Bethesda, MD 20889-5603; and <sup>†</sup>Department of Anatomy and Cell Biology, State University of New York Health Science Center at Brooklyn, Brooklyn, NY 11203

**ABSTRACT.** The adherence of undifferentiated <sup>51</sup>Cr-labeled HL-60 ( $0.5 \times 10^6$  HL-60 cells/well) cells was monitored on influenza virus-infected HUVEC monolayers. Whereas only  $3.0 \pm 1.6\%$  ( $n = 36$ ) of HL-60 cells adhered to uninfected HUVEC, adherence was increased to  $41.7 \pm 2.2\%$  ( $n = 6$ ),  $79.7 \pm 1.2\%$  ( $n = 6$ ),  $83.9 \pm 0.7\%$  ( $n = 6$ ), and  $84.4 \pm 0.5\%$  ( $n = 6$ ) on HUVEC infected for 7 h at a MOI of 1, 3, 6, and 9, respectively. In comparison, HL-60 cell adherence increased to 35% when HUVEC monolayers were stimulated with LPS (0.2–20  $\mu$ g) for 4 h. Increased adherence to infected HUVEC occurred at 5 h postinfection, peaked at 7 h, and was maintained at 24 h postinfection. Active virus and metabolically active endothelial cells were required to mediate the virus-induced adherence. E-selectin and ICAM-1 Ag were upregulated 78.3- and 4.1-fold, respectively, by LPS (0.02–20  $\mu$ g, 4 h) whereas virus infection (7 h) only increased these proteins 2.6- and 1.4-fold with a MOI  $\geq 16$ . Although the time courses of expression for both adhesion molecules after LPS treatment or virus infection were similar, the difference in the magnitude of upregulation suggests that virus-induced adherence is not a result of upregulation of E-selectin and ICAM-1. In contrast, surface expression of HA is involved in HL-60 cell adherence to virus-infected HUVEC because (1) the time course and magnitude of HA Ag expression paralleled the time course and magnitude of HL-60 cell adherence after virus infection of HUVEC; (2) HL-60 cell aggregates were absent on infected HUVEC monolayers in the presence of anti-HA; (3) HL-60 cells competed with RBC for infected endothelial cells stained for cellular HA Ag and (4) anti-HA abolished the virus-induced adherence. Furthermore, it appears that HL-60 cells are binding directly to HA because HL-60 cell adherence to a cell-free surface was increased if virus was prebound and neuraminidase treatment of HL-60 cells prevented the HL-60 cell adherence to influenza virus-infected endothelial monolayers. *Journal of Immunology*, 1993, 151: 310.

**L**eukocyte adherence to endothelial cells lining blood vessels is an integral part of an inflammatory response. Both *in vivo* (1) and *in vitro* (2–4) studies indicate that reactive oxygen species and proteolytic enzymes released at leukocyte-endothelial cell adherence sites produce endothelial cell injury. Endothelial cell injury,

in turn, has been implicated in the development of various vascular disorders, including atherosclerosis, vasculitis, and adult respiratory distress syndrome (5–7). In some of these inflammatory diseases, the presence of viral particles, viral antigens, and viral DNA has suggested that viral infections play a role in the progression of vascular disease (5, 8–10). Further support for this possibility has come from *in vitro* observations that cultured endothelial cells infected with HSV, CMV, adenovirus, or polio virus develop an increased adhesiveness to phagocytic leukocytes (7, 11–18).

Whereas few studies have examined the role of endogenous endothelial cell adhesion molecules, such as ICAM-1, E-selectin, and P-selectin, in virus-induced leukocyte-endothelial cell adhesion, their roles in cytokine-induced leukocyte adhesion have been well characterized (19–24). Furthermore, little is known about the role of viral

Received for publication October 16, 1992. Accepted for publication March 29, 1993.

The costs of publication of this article were defrayed in part by the payment of page charges. This article must therefore be hereby marked *advertisement* in accordance with 18 U.S.C. Section 1734 solely to indicate this fact.

<sup>1</sup> This work was supported by the Armed Forces Radiobiology Research Institute, Defense Nuclear Agency, under work unit 00020.

<sup>2</sup> Address correspondence and reprint requests to Address correspondence and reprint requests to Margaret Colden-Stanfield, Ph.D., Department of Physiology, AFRR, 8901 Wisconsin Avenue, Bethesda, MD 20889-5603

pathogen-derived molecules in either directly or indirectly mediating leukocyte-endothelial cell adhesion. In HSV-infected endothelial cells, the viral glycoprotein C molecule results in the local generation of thrombin, which then mediates the upregulation of P-selectin (25). Thus, in HSV-infected endothelial cells a viral glycoprotein indirectly mediates the increased leukocyte adherence.

In vitro influenza infection of endothelial cells also produces an increase in leukocyte adherence (26). Although the in vivo correlate of this observation is unclear, because influenza is commonly associated with respiratory epithelium, extrapulmonary manifestations have been reported. These manifestations include viremia (27–28) and, following fatal influenza pneumonia, recovery of the virus from the adrenal glands, heart, liver, meninges, and spleen (29–32). Thus, in vivo infection of endothelial cells is likely to occur during a disseminated influenza infection.

The purpose of this study was to further characterize influenza virus-induced leukocyte adherence to endothelial cell monolayers and to determine the mechanism underlying the increased adherence. We have demonstrated an increased adherence of HL-60 cells to influenza virus-infected HUVEC<sup>3</sup> monolayers as early as 5 h after infection. Whereas small increases in E-selectin and ICAM-1 Ag expression were noted in infected endothelial cells, these Ag played a minor role in the increased leukocyte adherence. Rather, our studies indicate that HL-60 cell adherence was mediated directly by the expression of the influenza virus glycoprotein HA on the surface of the infected endothelium.

## Materials and Methods

### Cell culture

Endothelial cells were dislodged from the vessel wall of the umbilical vein from human umbilical cord (Holy Cross Hospital, Bethesda, MD) by incubating with a 1% collagenase/PBS solution (Type II, Worthington Biochemical Corp., Freehold, NJ) for 15 min at 37°C. Cells were sloughed off by kneading the cord and flushing the lumen with MCDB107 medium (American Biorganics, Inc., N. Tonawanda, NY). Complete MCDB107 containing 10% heat-inactivated FCS (Hyclone Laboratories, Inc., Logan, UT), 100 U/ml penicillin, 100 µg/ml streptomycin, 2 mM glutamine (all from GIBCO Laboratories, Grand Island, NY), 100 µg/ml heparin (Sigma, St. Louis, MO), and 50 µg/ml endothelial cell growth supplement (H-Neurext, Upstate Biotechnology, Inc., Lake Placid, NY) was added to cells that were then centrifuged at 1500 rpm for 5 min to pellet cells. Pellets were resuspended in complete

MCDB107, plated in 100-mm collagen-coated (Type II, Collaborative Research, Bedford, MA) tissue culture dishes, and placed in a 37°C, 95% air/5% CO<sub>2</sub>-humidified incubator. Purity of our endothelial cell population was confirmed by the characteristic "cobblestone," nonoverlapping morphology of confluent monolayers (33, 34) and the presence of uniformly distributed acetylated low-density lipoprotein identified with the fluorescence probe 1,1'-diiododecyl-1-3-3'-3'-tetramethyl-indocarbocyanine perchlorate (Biomedical Technologies, Inc., Stoughton, MA) as previously described (35). Experimental data were obtained from HUVEC in their second to sixth passages, which were 1 to 2 days postconfluent.

HL-60 cells (American Type Culture Collection, Rockville, MD) were used in the undifferentiated state to assess leukocyte-endothelial cell adherence. The cell line was grown in suspension with RPMI 1640 (GIBCO) containing 10% nonheat-inactivated FCS, 100 U/ml penicillin, 100 µg/ml streptomycin, 200 µg/ml neomycin, and 2 mM glutamine. HL-60 cells used in the adhesion assay were in their 23rd to 27th passages.

### mAb

Murine mAb H18/7 (IgG<sub>2a</sub>, a gift from Dr. M. Gimbrone, Brigham & Women's Hospital, Boston, MA), binds to a functional epitope on the HUVEC surface protein ELAM-1 (E-selectin). Murine mAb 84H10 (IgG<sub>2a</sub>), donated by Dr. S. Shaw (National Cancer Institute, Bethesda, MD), recognizes an epitope on the HUVEC surface protein ICAM-1. Murine mAb H17-L19 (IgG1), which blocks the RBC binding site on the globular head of the viral glycoprotein HA, was produced from a hybridoma provided by Dr. W. Gerhard (Wistar Institute, Philadelphia, PA). Control murine mAb, W6/32 (IgG<sub>2a</sub>, Accurate Chemical & Scientific Corporation, Westbury, NY), which recognizes an HLA-A,B,C determinant constitutively expressed on HUVEC, was used as a nonrelevant binding antibody.

### Virus preparation and infection

The WSN (H1N1) strain of influenza virus type A was grown in the MDCK cell line as previously reported (36). Stock virus was titered at 2–8 × 10<sup>9</sup> plaque-forming U/ml and stored in liquid nitrogen until needed. Endothelial cells were infected by adding influenza virus (MOI = 1, unless otherwise noted) in complete MCDB107 to HUVEC monolayers. After 1 h of adsorption, the medium was aspirated and rinsed once before fresh complete MCDB107 was added to each well.

### Assessment of cell viability

Cell viability was assessed after virus infection and/or LPS treatment of the HUVEC monolayers by performing a cytotoxicity assay using a colorimetric kit (LK-100, Proteins

<sup>3</sup> Abbreviations used in this paper: HUVEC, human umbilical vein endothelial cell; HL-60, human promyelocytic leukemia cell; HA, hemagglutinin; MOI, multiplicity of infection; CPE, cytopathic effects; TCID<sub>50</sub>, 50% tissue culture infectious dose.

Table 1  
Endothelial cell viability after virus infection and/or LPS treatment<sup>a</sup>

Treatment		% Cytotoxicity
Naive HUVEC (spontaneous release)		5.2 ± 0.7 (10)
LPS-treated HUVEC		3.9 ± 0.6 (5)
Virus-Infected HUVEC	7 to 9 h postinfection	24 h postinfection
MOI 0.1		28.2 ± 3.2 (5)*
MOI 1	3.9 ± 0.6 (9)	20.4 ± 1.2 (5)*
MOI 8	3.3 ± 0.9 (5)	30.3 ± 0.6 (5)*
MOI 1 + LPS 0.5 µg	2.7 ± 0.5 (5)	

<sup>a</sup> Data are expressed as the mean ± SEM with the number of observations in parenthesis. HUVEC monolayers were either mock-infected, infected, or infected and LPS-treated. Cytotoxicity was assessed as described in the *Materials and Methods*.

The symbol \* denotes a statistical difference between spontaneous release (naive HUVEC) and the test group ( $p \leq 0.05$ ).

International, Rochester Hills, MI) that equates the release of lactate dehydrogenase to the number of injured cells. At various times after virus infection (MOI 0.1, 1, or 8) and/or 4 h after LPS treatment (0.5 µg) of HUVEC monolayers plated in 96-well plates, 100 µl of supernatant from each well was mixed with 100 µl of substrate mixture. After 30 min, color development was stopped with 1 N HCl, and absorbance was read at 492 nm wavelength on a Titertek ELISA plate reader (ICN Biomedicals, Inc., Costa Mesa, CA). Supernatants from control HUVEC were used to measure the spontaneous release of the enzyme, whereas supernatants from HUVEC exposed to a lysing reagent were used to determine the maximum release of the enzyme. The following equation was used to calculate percentage of cytotoxicity:

$$\% \text{ cytotoxicity} = \frac{\text{exp. abs.} - \text{spont. abs.}}{\text{max. abs.} - \text{spont. abs.}} \times 100$$

As shown in Table I, there was no measurable cytotoxicity 7 to 9 h after virus infection. In addition, a 4-h LPS treatment or a combined virus infection (7–9 h) and 4-h LPS treatment did not affect viability of the HUVEC monolayers. Cytotoxicity (20–30%) was observed only 24 h after virus infection of HUVEC. Therefore, experiments were performed 7 h after virus infection except when time courses were generated.

#### Virus infectivity titrations

To determine the susceptibility of HUVEC monolayers to influenza virus infection, infectivity was measured by quantitating the dilution of virus at which 50% of the infected cultures possessed CPE such as cell rounding, detachment, or death (37–38). HUVEC seeded in 96-well plates were infected with 100 µl of serial 10-fold dilutions of the virus in cold MCDB107. Wells with uninfected HUVEC were treated identically except that the medium

contained no virus. After a 1-h adsorption period in a 37°C 5% CO<sub>2</sub>-humidified incubator, the medium was aspirated and replenished, and cultures were returned to the incubator. Daily readings of CPE were recorded with the assay being terminated on day 7. The observed viral CPE was corroborated using a hemadsorption assay with human RBC (39) to detect surface viral HA protein. The TCID<sub>50</sub> was determined by the method of Reed and Muench (40). In viral titrations, the hemadsorption endpoint was compared with the CPE endpoint. Wells with visible CPE were always positive by hemadsorption, and wells with no signs of CPE were always negative.

#### Adhesion assay

HUVEC (30 × 10<sup>4</sup> cells/well) were seeded in collagen-coated 24-well plates 48 h before the confluent monolayers were virus infected. For comparison, other HUVEC monolayers were treated with LPS, a known promoter of leukocyte-endothelial cell interactions (41–44). At various times after infection or LPS treatment, <sup>51</sup>Cr-labeled HL-60 cells (0.5 × 10<sup>6</sup> cells/well) suspended in Dulbecco's MEM/5% FCS were added to HUVEC monolayers for 30 min at 37°C in a 5% CO<sub>2</sub>-humidified incubator. Unbound HL-60 cells were aspirated, and the endothelial cell monolayers were washed five times with assay medium before the remaining adherent cells were lysed with 1 N NH<sub>4</sub>OH. The lysate and a second wash with NH<sub>4</sub>OH were transferred to vials for subsequent radioanalysis using an LKB 1282 COMPUGAMMA Counter CS (LKB Wallac, Turku, Finland). The percentage of HL-60 cell adherence was calculated as:

% adherence

$$= \frac{\text{cpm test HL-60 cells} - \text{cpm NH}_4\text{OH}}{\text{cpm total HL-60 cells} - \text{cpm NH}_4\text{OH}} \times 100$$

The effects of endothelial-directed mAb on HL-60 adherence to uninfected or virus-infected HUVEC were determined by incubating HUVEC with saturating concentrations (90 µg/ml) of endothelial cell-directed mAb for 30 min at 37°C before and during the adhesion assay.

#### Detection of cell surface antigens

To measure surface Ag expression on HUVEC monolayers after influenza virus infection or LPS treatment, 2% paraformaldehyde-fixed (15 min at room temperature) HUVEC monolayers in collagen-coated 96-well plates were first incubated with PBS/1% BSA for 30 min at room temperature to block nonspecific binding. Each subsequent step of the ELISA was carried out at room temperature with three washes of PBS/1% BSA between steps. The fixed monolayers were incubated in turn with a saturating concentration of the test mAb and a peroxidase-conjugated

goat anti-mouse IgG (Sigma) for 1 h. *o*-Phenylenediamine (0.4 mg/ml)/0.012% hydrogen peroxide in a 0.05/0.025 M phosphate/citrate buffer, pH 5.0, was added to each well. Color development was stopped with 3 M H<sub>2</sub>SO<sub>4</sub> at 20 min, and the OD was read at 492 nm wavelength. The degree of specific Ag expression was calculated by subtracting non-specific binding of the secondary antibody from all test values.

#### Colocalization of cell aggregates and HA Ag

A modification of the hemadsorption assay was used to confirm that RBC and/or HL-60 cell aggregates were binding to infected endothelial cells. Infected HUVEC monolayers seeded on fibronectin-coated (Collaborative Research, Inc., Bedford, MA) glass coverslips (Bellco Biotechnology Vineland, NJ) were incubated for 30 min at 37°C in a 5% CO<sub>2</sub>-humidified incubator with either RBC (human Type O, 0.5% in Gey's balanced salt solution), HL-60 cells (0.5 × 10<sup>6</sup> cells), or medium lacking cells. Cultures were rinsed of nonadherent cells, and then the second cell type was added to some cultures for 30 min before cultures were washed of nonadherent cells. The remaining endothelial cell monolayers with adherent RBC and/or HL-60 cells were fixed with 2% paraformaldehyde in PBS (7.4) for 30 min on ice. Cellular HA Ag was fluorescently monitored by permeabilizing the fixed HUVEC monolayers in -20°C acetone for 3 min before rinsing in PBS/50 mM NH<sub>4</sub>Cl and storing overnight at 4°C. The monolayers were then washed in PBS/1% BSA for 30 min at room temperature, incubated with intact anti-HA (H17-L19, 1:20) for 1 h at room temperature, rinsed with PBS/1% BSA, and incubated with a rhodamine-conjugated goat anti-mouse IgG (1:100, Sigma). After 1-h incubation at room temperature in the dark with the secondary antibody, HUVEC monolayers were washed, monitored for fluorescence with rhodamine optics (546 to 610 nm excitation/590 nm emission/580 nm dichroic mirror, Carl Zeiss, Inc., Thornwood, NJ), and photographed on Ektachrome Tungsten 160 film (Eastman Kodak Co., Rochester, NY).

#### Data analysis

To test the effect of virus infection of HUVEC monolayers on HL-60 cell adherence and Ag expression the Student's *t*-test was used. The symbol \* denotes a statistical difference ( $p \leq 0.05$ ) between test and corresponding control groups.

### Results

#### Susceptibility of HUVEC monolayers to influenza virus infection

The ability of influenza virus to infect HUVEC monolayers and produce CPE was monitored over a 7-day period.

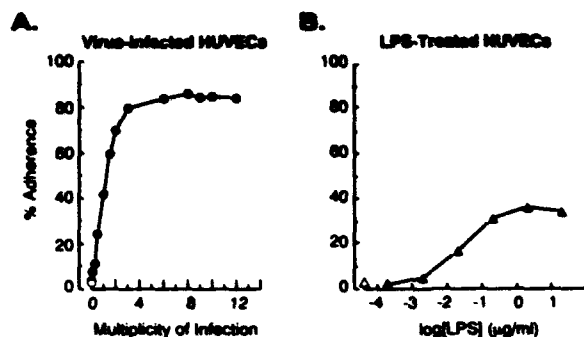


**FIGURE 1.** Dose response of HL-60 cell adherence to HUVEC monolayers (A) influenza virus infected for 7 h or (B) LPS treated for 4 h. HUVEC monolayers were exposed to various concentrations of virus or LPS, and a standard adhesion assay was performed as described in *Materials and Methods*. Each point represents the mean  $\pm$  SEM of six replicates in a representative experiment of three separate experiments. In this graph and all subsequent graphs, error bars are omitted when smaller than the size of the symbol. The open symbols in all figures indicate control HUVEC.

Endothelial cytoplasmic vacuolization was detected in all HUVEC cultures ( $n = 8$ ) infected with a  $10^{-6}$  dilution on day 3 after infection, whereas cellular detachment was evident on days 4 to 7 with that same dilution. However, only 3 of 8 wells and 1 of 8 wells showed evidence of CPE on days 3 to 7 for HUVEC cultures infected with  $10^{-7}$  and  $10^{-8}$  dilutions, respectively. A  $10^{-5.6}$  TCID<sub>50</sub>/ml dilution was calculated to be the dilution at which 50% of the HUVEC cultures would possess CPE. In comparison, MDCK epithelial cells, which are known to fully support influenza virus replication, have a  $10^{-8}$  TCID<sub>50</sub>/ml with a comparable viral pool.

#### Characterization of HL-60 cell adherence to influenza virus-infected or LPS-treated HUVEC

The adherence of HL-60 cells to uninfected control HUVEC monolayers was  $3.0 \pm 1.6\%$  (Fig. 1 A). In contrast, HL-60 cell adherence to influenza virus-infected HUVEC monolayers monitored 7 h postinfection was increased in a concentration-dependent manner. Adherence was saturated with 83% of HL-60 cells binding to endothelial monolayers infected with a MOI  $\geq 4$  (Fig. 1 A). Microscopic inspection of monolayers indicated that HL-60 cells bound in both singlets and aggregates to infected HUVEC monolayers. A similar virus-induced adherence occurred with cAMP-differentiated HL-60 cells and freshly isolated human neutrophils (data not shown). This virus-induced adherence differed from the adhesion produced by treating HUVEC for 4 h with saturating concentrations of LPS, where HL-60 cells adhered as singlets, and adherence was increased to only 35% (Fig. 1 B).

HL-60 cell adherence to LPS-treated HUVEC reached maximal levels by 3 h, remained elevated through 7 h, and

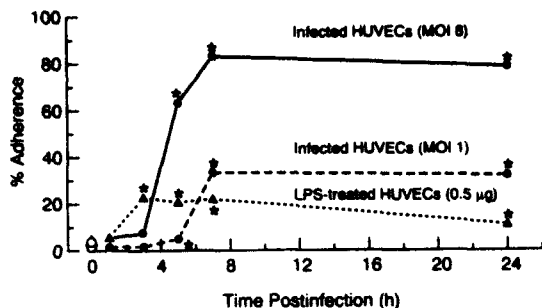


**FIGURE 2.** Time course of HL-60 cell adherence to virus-infected or LPS-treated HUVEC monolayers. HL-60 cell adherence to HUVEC monolayers was monitored at various times after virus infection (MOI 1 or 8) or LPS treatment (0.5  $\mu$ g). Each point is the mean  $\pm$  SEM of six replicates in a representative experiment of three separate experiments.

decreased 49% after 24 h of LPS treatment (Fig. 2). Increased adherence to infected HUVEC occurred at 5 h postinfection, peaked at 7 h, and remained at maximal levels 24 h after infection regardless of the virus titer used (Fig. 2).

To determine if viable influenza virus was required to stimulate HL-60 cell adherence to HUVEC monolayers, the adhesion assay was performed with active and UV-inactivated virus. Exposure of the virus to UV light for 30 min before addition to HUVEC monolayers abolished the increase in HL-60 cell adherence (data not shown). Furthermore, HL-60 cell adherence to paraformaldehyde-fixed HUVEC that were subsequently infected with active virus failed to show an increased adherence (Fig. 3, striped bar). In contrast, HUVEC fixed 7 h after infection with active virus displayed an 8.6-fold increase in leukocyte adherence (Fig. 3, filled bar). Fixing HL-60 cells before performing the adhesion assay with infected HUVEC did not prevent the virus-induced adherence (data not shown). Thus, the interaction of metabolically active endothelial cells and live virus was required for the increased HL-60 cell adherence, while metabolically active HL-60 cells were not required.

#### Surface expression of endothelial adhesion molecules

The dose-response of E-selectin and ICAM-1 surface Ag expression induced by either influenza virus infection or LPS treatment is shown in Figure 4. While the ICAM-1 Ag was expressed constitutively on the surface of uninfected endothelial cells, the E-selectin Ag was not. ICAM-1 and E-selectin expression was increased 1.1- and 1.4-fold, respectively, with an MOI of 1, and maximally increased 1.3- and 2.6-fold with an MOI  $\geq$  16 (Fig. 4 A). As a comparison, the surface expression of ICAM-1 and E-selectin was monitored after a 4-h treatment of HUVEC with LPS (Fig. 4 B). ICAM-1 and E-selectin Ag increased by 4.1- and 78.3-fold, respectively, after exposure to LPS (0.02–20  $\mu$ g). Constitutively expressed HLA-A,B,C Ag, monitored by the

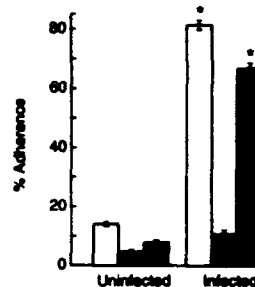


**FIGURE 3.** Effect of fixation on HL-60 cell adherence to virus-infected HUVEC monolayers. The adhesion assay was performed with HUVEC monolayers that were either mock- or virus-infected (MOI 8) before (*solid bars*) or after (*striped bars*) fixing with 2% paraformaldehyde for 5 min and washed twice. The *open bars* represent unfixed HUVEC monolayers. A small decrease in antigenicity produced by fixation probably caused the slight decline in HL-60 cell adherence to fixed uninfected HUVEC monolayers. Each *bar* is the mean  $\pm$  SEM of six replicate wells in a typical experiment of three separate experiments.

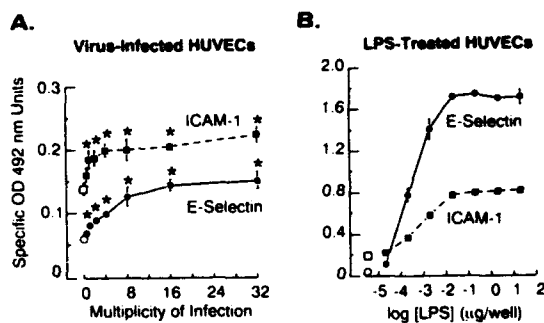


**FIGURE 4.** Dose response of surface Ag expression on HUVEC monolayers (A) virus infected for 7 h or (B) LPS treated for 4 h. HUVEC were exposed to various concentrations of virus or LPS, and surface ICAM-1 and E-selectin expression was quantitated by the ELISA assay described in *Materials and Methods*. Note the difference in the ordinate scales. Each *point* is the mean  $\pm$  SEM of quadruplicate wells of a representative experiment of two separate experiments. Ag expression for both adhesion molecules was significantly greater than control Ag expression, (*open symbols*) at LPS concentrations  $\geq$  0.0002  $\mu$ g.

W6/32 antibody of the same isotype, was not altered by LPS treatment or virus infection of HUVEC (data not shown).

The time course of Ag expression of both adhesion molecules after virus infection or LPS treatment was followed using a virus titer and an LPS dose shown to induce E-selectin and ICAM-1 (Fig. 5). E-selectin surface Ag was induced on virus-infected HUVEC as early as 1 h postinfection, peaked between 5 and 7 h postinfection, and began to decrease at 24 h postinfection (Fig. 5 A). Virus-induced ICAM-1 expression did not begin until 5 h and continued to increase by 24 h postinfection. A comparison of the data

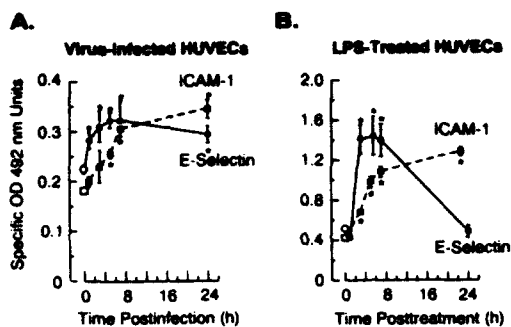


**FIGURE 5.** Time course of surface antigen expression on HUVEC monolayers (A) virus infected with an MOI of 1 or (B) treated with 0.5  $\mu$ g LPS. ICAM-1 and E-selectin expression was quantitated at various times after virus infection or LPS treatment of HUVEC monolayers. Note the difference in the ordinate scales. Each point is the mean  $\pm$  SEM of quadruplicate wells in a typical experiment of three separate experiments.

on virus-infected HUVEC (Fig. 5 A) to that obtained from LPS-treated HUVEC (Fig. 5 B) indicates that the magnitude of the increase in endothelial adhesion molecules induced by virus infection follows a similar time course but was less than 30% of the expression after LPS treatment.

It was possible that influenza virus infection of HUVEC reduced host protein synthesis, thereby producing only small increases in E-selectin and ICAM-1 Ag. To test this possibility, HL-60 cell adherence and adhesion molecule Ag expression was monitored after a combined virus infection and LPS treatment protocol. Five h after HUVEC monolayers were infected with influenza virus, the infected cells were exposed to LPS (0.5  $\mu$ g) for 4 h. This time point was chosen because at 5 h postinfection cells will be actively synthesizing and packaging viral proteins (39, 45). As shown previously, HL-60 cell adherence to HUVEC monolayers was enhanced 36-fold after virus infection, and 4 h of LPS treatment alone produced a 13-fold increase in adherence (Fig. 6 A). HUVEC exposed to a combination of influenza virus and LPS, however, showed an additive effect with a 46-fold increase in HL-60 cell adherence compared to control conditions (Fig. 6 A), indicating that prior virus infection did not significantly inhibit LPS-induced HL-60 cell adherence.

ICAM-1 and E-selectin Ag expression was quantitated under the same experimental conditions. While virus infection alone only increased ICAM-1 and E-selectin expression by 1.3- and 2.6-fold, respectively, LPS treatment produced a 2.7- and 67-fold respective increase in these surface proteins (Fig. 6 B). ICAM-1 and E-selectin Ag expression continued to be upregulated by LPS-treatment after virus infection of HUVEC. However, the actual 2.3- and 60.2-fold respective increase in ICAM-1 and E-selectin Ag following the combined treatment protocol was 43 and 14%, respectively, lower than the expected values would

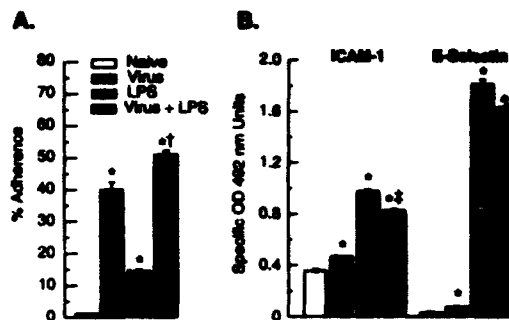


**FIGURE 6.** (A) HL-60 cell adherence to and (B) surface Ag expression on HUVEC monolayers that were either control (naive), virus infected (MOI 1), LPS treated (0.5  $\mu$ g), or infected and LPS treated. The combined treatment protocol consisted of HUVEC monolayers being infected for 5 h before they were LPS treated for 4 h. Each bar is the mean  $\pm$  SEM of (A) six replicates and (B) four replicates of two separate experiments. \* denotes a statistical difference ( $p \leq 0.05$ ) between test and corresponding control groups. † signifies a significant difference between the combined treatment group and the infected group ( $p \leq 0.05$ ). ‡ indicates a statistical difference between the combined treatment group and the LPS group ( $p \leq 0.05$ ).

have been if the effects of LPS treatment and viral infection were additive. Nonetheless, the small reduction in ICAM-1 and E-selectin levels by infection cannot account for the failure of virus infection to maximally upregulate these molecules.

#### Role of the influenza viral glycoprotein HA in virus-induced adherence

The hemadsorption assay and immunofluorescence techniques demonstrated that HL-60 cells bind and aggregate to endothelial cells that stain positive for the HA Ag (Fig. 7). In fact, HL-60 cells competed with RBCs for binding to HA-positive endothelial cells, suggesting that HL-60 cells bound specifically to the HA protein on the surface of the infected HUVEC (Fig. 7 C). To determine if sialic acid residues on the surface of HL-60 cells interacted with HA protein budding on the infected HUVEC monolayer, we treated HL-60 cells with neuraminidase to cleave sialic acid residues and quantitated adherence to virus-infected HUVEC monolayers. While HL-60 cell adherence to uninfected HUVEC monolayers was not affected by prior neuraminidase treatment, virus-induced adherence was inhibited by 98% (Fig. 8).

As illustrated in Fig. 9, HA Ag expression was monitored on HUVEC monolayers 7 h after infection with various titers of influenza virus. As expected, there was minimal HA expression on the surface of uninfected HUVEC monolayers. However, infection of the endothelial cell monolayers dose-dependently increased HA Ag with a maximal 12.7-fold increase at an MOI  $\geq 16$ , which was shown previously to saturate HL-60 cell adherence. HA expression

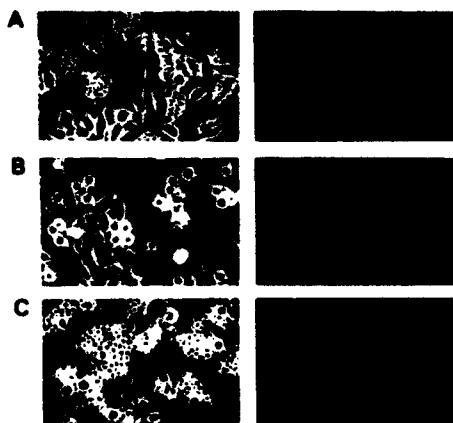


**FIGURE 7.** Bright field (left panel) and fluorescent (right panel) micrographs examining colocalization of (A) RBC, (B) HL-60, or (C) RBC + HL-60 aggregates and cellular HA Ag 7 h after influenza virus infection (MOI 24) of HUVEC monolayers. Virus-infected HUVEC monolayers were incubated with RBC, HL-60 cells, or RBC first and then HL-60s or vice versa before they were fixed and stained for cellular HA Ag as described in *Materials and Methods*. Bar = 45  $\mu$ m.

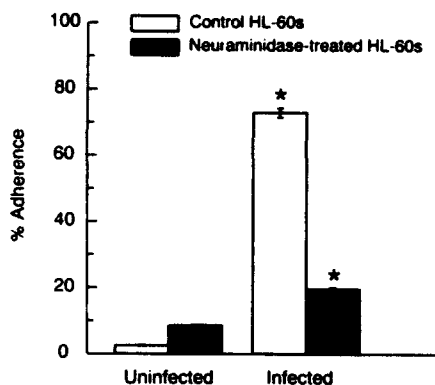


**FIGURE 8.** Effect of neuraminidase treatment of HL-60 cells on adherence to virus-infected HUVEC monolayers. HL-60 cells were exposed to neuraminidase (0.1 U, from *Vibrio cholerae*, Sigma, St. Louis) in RPMI/5% FCS for 30 min at 37°C with gentle agitation, washed several times, and then used in the adhesion assay to quantitate adherence to HUVEC monolayers infected (MOI 1) for 7 h. Each bar is the mean  $\pm$  SEM of five to six replicate wells in a representative experiment of two separate experiments.

was similar with titers as high as an MOI of 90 (data not shown). This viral protein was not apparent on infected HUVEC until 5 h postinfection, peaked at 7 h, and remained maximal at 24 h postinfection, which paralleled the time course of HL-60 cell adherence to the infected endothelium (Fig. 10). HA Ag expression was not evident on HUVEC treated with LPS for 4 h at concentrations that maximally induced expression of E-selectin and ICAM-1 Ag (data not shown).

To directly demonstrate the role of surface HA in the virus-induced adherence, two experimental protocols were performed. First, uninfected and infected HUVEC were in-

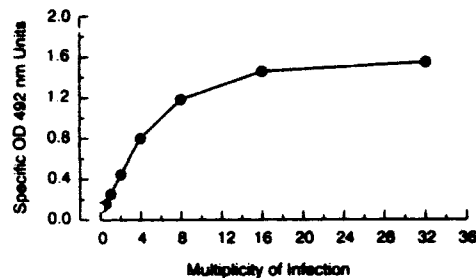


**FIGURE 9.** Dose response of surface HA antigen expression on infected HUVEC monolayers. Seven hours after exposure of HUVEC monolayers to various titers of influenza virus, monolayers were fixed, and HA Ag expression was quantitated using H17-L19 (anti-HA) in the ELISA assay described in *Materials and Methods*. Each point is the mean  $\pm$  SEM of quadruplicate wells in a representative experiment of two separate experiments. HA Ag expression was significantly different from control Ag expression at MOI  $\geq$  1.

cubated with F(ab')<sub>2</sub> fragments of anti-HA, intact anti-E-selectin, anti-ICAM-1, and/or anti-HLA before and during the adhesion assay. The presence of anti-HA alone blocked the virus-induced HL-60 cell adherence by 95% while it had no effect on basal adherence (Fig. 11). In addition, no HL-60 cell aggregates were visible on infected HUVEC monolayers in the presence of anti-HA. While the combined presence of antibodies against HA, E-selectin, and ICAM-1 inhibited the virus-induced adherence by 96.5%, there was no specific effect of anti-E-selectin and anti-ICAM-1 on induced adherence since exposure to these two antibodies inhibited virus-induced adherence to the same extent (19%) as the nonrelevant binding anti-HLA (Fig. 11).

Second, the adhesion assay was performed with <sup>51</sup>Cr-labeled HL-60 cells in the absence of HUVEC monolayers on polylysine-coated wells without and with bound influenza virus. Adherence of HL-60 cells to polylysine-coated wells was minimal with bound singlets (Fig. 12). However, when HL-60 cells were added to wells that had the virus bound to the surface, there was a threefold increase in adherent HL-60 cells, with some cells binding as aggregates (Fig. 12).

## Discussion

Viral infections, including influenza virus infections, have been associated with leukopenia (46–50). One of the possible causes for this virus-induced leukopenia may be adherence of circulating leukocytes to virus-infected endothelial cells lining blood vessels since as both enteroviruses that cause an acute lytic infection and adenoviruses that produce a chronic, slowly lytic infection of endothelial cell monolayers also have been shown to enhance granulocyte adherence to endothelial cell monolayers (11–12). In this study we demonstrate that infection of cultured endothelial

**FIGURE 10.** Time course of HA Ag expression on infected HUVEC monolayers. At various times after virus infection (MOI 1) of HUVEC monolayers, surface HA Ag expression was measured. Each point is the mean  $\pm$  SEM of quadruplicate wells in a representative experiment of two separate experiments. Inset: Time course of HL-60 cell adherence to virus-infected (MOI 1) HUVEC monolayers (same as in Fig. 2).

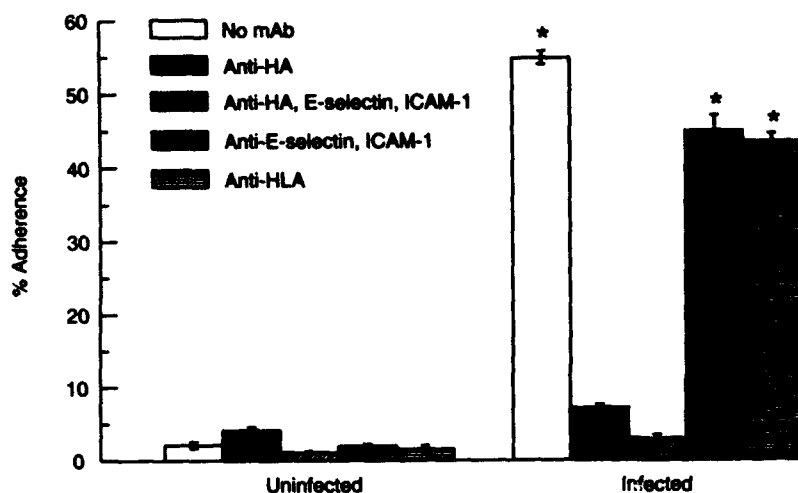
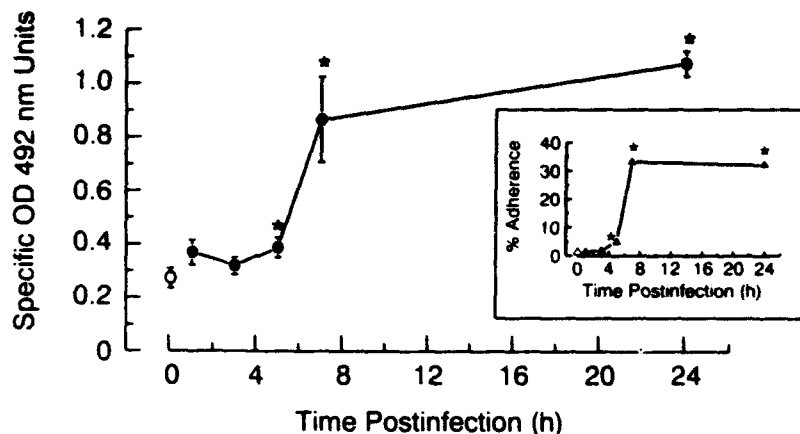


**FIGURE 11.** Effect of endothelial-directed antibodies on HL-60 cell adherence to virus-infected HUVEC monolayers. Uninfected or infected (MOI 1, 7 h postinfection) HUVEC monolayers were exposed to no antibody, anti-HA (H17-L19), anti-E-selectin (H18/7), anti-ICAM-1 (84H10), and/or anti-HLA (W6/32) before and during the adhesion assay. Each bar is the mean  $\pm$  SEM of four to five replicate wells in a representative experiment of two separate experiments.

cells with a common human pathogen, influenza virus type A, also promotes leukocyte adherence and that the molecule underlying the increased adherence is the influenza viral protein HA expressed on the surface of infected endothelial cells.

In contrast to the Victoria/75 (H3N2) strain of influenza virus type A, which did not infect human venous or bovine arterial endothelium at a low virus titer (MOI 0.1–0.3) (51), the WSN (H1N1) strain in our study produced a slowly lytic infection in HUVEC as evidenced by the time of onset of CPE. Hemadsorption of RBC and immunofluorescence indicated that most of the endothelial cells were infected with virus under our experimental conditions. Moreover, we have shown previously, using electron microscopic techniques, that this strain of influenza buds from the apical surface of endothelial cells (52). The increase in HL-60 cell adherence to infected endothelium required metabolically active endothelial cells because fixing the HUVEC monolayers before exposing them to the virus-containing medium abolished the increase in HL-60 cell adherence. Conversely, fixing HL-60 cells did not alter the virus-induced adherence. A similar inhibition of induced leukocyte ad-

herence occurs when endothelial cells are fixed before cytokine or LPS treatment (53–54).

The time course for HL-60 cell adherence to influenza virus-infected HUVEC was found to be similar to time courses of leukocyte adherence to endothelial cells infected with other viruses. HL-60 cell adherence to endothelial cell monolayers was modulated by influenza virus infection with an increase beginning at 5 h, peaking at 7 h, and lasting 24 h postinfection. Infection of endothelial cells with herpes viruses has been shown to enhance human neutrophil adherence as early as 4 h postinfection, with plateaus between 18 and 32 h postinfection (7, 13, 15, 17). Increased monocyte adherence to endothelial cells also occurs within 4 h of exposure to HSV 1 (16–17, 25) and was observed 25 h after either HSV (25) or CMV infection (17).

Influenza virus infection produced a robust 28-fold increase in HL-60 cell adherence under similar infection protocols (MOI 24) or with lower virus titers (MOI 1, ninefold increase) compared to the small twofold to threefold increase in leukocyte adherence observed in endothelial cells infected with CMV (17) and HSV (13, 25). This discrepancy in magnitude of response between our findings and

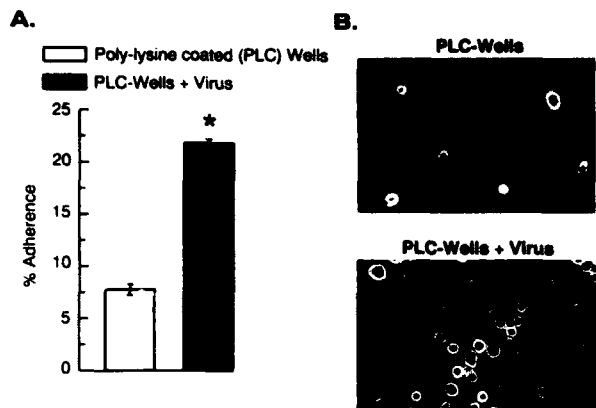


**FIGURE 12.** HL-60 cell adherence to polylysine-coated wells in the absence and presence of bound influenza virus. Wells were coated with polylysine (1 mg/ml) in Hank's balanced salt solution for 5 min, rinsed with deionized water, and allowed to dry. In some wells a high titer of virus (MOI 100) was added for 30 min at 37°C. After removing unbound virus,  $^{51}\text{Cr}$ -labeled HL-60 cells ( $2 \times 10^5$  cells) were added to the wells for the adhesion assay to proceed as described in *Materials and Methods*. (A) Each bar is the mean  $\pm$  SEM of five replicate wells in a representative experiment of two separate experiments. (B) Bright field micrographs of HL-60 cells bound to (upper panel) polylysine-coated wells and (lower panel) virus- and polylysine-coated wells. Same scale as in Fig. 7.

other studies may reflect the different leukocytes used in the various studies inasmuch as human neutrophils, monocytes, U937 cells, and HL-60 cells may exhibit different surface integrin profiles (55–57). Alternatively, these differences may be due to different mechanisms by which viral pathogens enhance leukocyte adherence. For example, the 1.4-fold increase in neutrophil adherence to HUVEC infected with CMV appears to be due, in large part, to the upregulation of surface ELAM-1 (E-selectin), because it was largely inhibited by an antibody against ELAM-1 (18). In contrast, both a soluble factor released from HSV-infected HUVEC (17) and a thrombin-dependent increase in GMP-140 (P-selectin) on the surface of infected HUVEC (25) have been implicated in the HSV-induced enhancement of monocyte binding.

In our studies, influenza virus infection of HUVEC monolayers produced small increases in two endothelial adhesion molecules, E-selectin and ICAM-1. While the magnitude of these increases was smaller, the time courses of upregulation of these adhesion molecules were similar to that produced after LPS or cytokine stimulation of HUVEC monolayers (41–44). However, the inability of antibodies against E-selectin and ICAM-1 to specifically block the increase in HL-60 cell adherence strongly suggests that these adhesion molecules play only a minor role or no role in the influenza virus-induced adherence and that other endothelial cells or viral proteins are involved. It is noteworthy that although ICAM-1 expression is also in-

creased on parainfluenza virus-infected airway epithelial cells, an antibody against ICAM-1 has no significant effect on parainfluenza-induced neutrophil adherence (58). In HSV-infected HUVEC, neutrophil adherence is indirectly dependent on the surface expression of the herpes virus glycoprotein. That is, the surface expression of the herpes virus glycoprotein C induces the local generation of thrombin and subsequent upregulation of GMP-140 (13, 25). It is unlikely that GMP-140 upregulation plays a role in HL-60 cell adherence to influenza-infected HUVEC because previous studies have demonstrated that, unlike neutrophils, undifferentiated HL-60 cells do not bind to GMP-140 (59).

Rather than implicating the upregulation of an endogenous endothelial cell adhesion molecule, several observations indicate that the expression of the influenza virus glycoprotein HA on the endothelial surface mediates the increased binding of HL-60 cells to infected HUVEC. First, the time course and dose response for HA Ag expression parallels that of HL-60 cell adherence to infected HUVEC monolayers. Second, HL-60 cell aggregates were absent on infected HUVEC monolayers in the presence of anti-HA. Finally, anti-HA abolished HL-60 cell adherence to influenza virus-infected endothelial monolayers. Furthermore, HA appears to serve directly as a binding site for HL-60 cells, inasmuch as leukocyte adherence to a cell-free surface was increased if virus was prebound, and the ability of neuraminidase treatment of HL-60 cells to cleave sialic residues actually prevented the virus-induced adherence. Thus, like HSV-infected HUVEC, a viral protein is also involved in the influenza virus-stimulated increases in HL-60 cell adherence, but, unlike HSV-infected endothelial cells, surface expression of a viral protein directly mediates leukocyte adherence.

We have described a similar direct binding between leukocytes and the viral protein HA on epithelial cells (MDCK) infected with either the same WSN (H1N1) strain (60) or the A/PR8 (H1N1) strain of influenza virus (unpublished data). While the interactions of influenza with epithelial cells, and in particular the respiratory epithelium, have been well studied, relatively little is known about the effect of influenza virus on other tissues in the body. In vitro studies indicate that neutrophils, which accumulate during the early stages of an influenza infection, are capable of transporting influenza virions on the surface of and within phagocytic vacuoles from the luminal to the abluminal surface of an epithelium, and thus, may play a role in the spread of infection (61). Viremia has been documented in individuals in the 1 to 3 day incubation period before the onset of symptoms (27–28) and in individuals with uncomplicated influenza infection (62) as well as severe influenza pneumonia (30–32). During viremia and disseminated infection, it is likely that influenza infects the endothelia lining the vessels of the respiratory system and of other organs.

In vivo, influenza virus binding to sialic acid residues may mediate leukocyte rolling and/or stable adhesion. Leukocyte rolling, an early step in the inflammatory response, can be mediated by GMP-140 binding to a sialylated carbohydrate ligand with a Lewis x component (63) and presumably occurs because lectin-carbohydrate interactions possess fast on-and-off rates in the range of  $10^5$  to  $10^6$  M<sup>-1</sup> s<sup>-1</sup> and 2.3 to 56 s<sup>-1</sup>, respectively (64–66). Because very fast kinetics have been described for the interaction of influenza virus with HL-60 cells and other cultured cells ( $k_{+1} > 10^{10}$  M<sup>-1</sup> s<sup>-1</sup> and  $k_{-1} \leq 0.004$  s<sup>-1</sup>; (67)), and the  $K_D$  of virus binding to sialic acid residues is  $\geq 1$  mM (68 to 69) influenza virus infection of endothelial cells in vivo may similarly mediate leukocyte rolling. In our study, weak binding (sensitive to vigorous wash steps) was observed between HL-60 cells and influenza virus in a cell-free system. However, we observed a tighter binding (maintained after several washes) between HL-60 cells and virus-infected endothelial cells suggesting that an additional mechanism mediates this interaction. In contrast to RBC adherence, raising the temperature from 4°C to 37°C increases HL-60 cell adherence (data not shown) and neutrophil binding (39) to endothelial and epithelial cell monolayers, respectively. This suggests that the interaction between HA and its sialylated ligand on leukocytes is different from the binding between HA and RBC. Therefore, it is plausible that under flow conditions virus infection mediates not only HA-related leukocyte rolling, but subsequent facilitation of a more stable integrin-like adhesion.

In summary, we have demonstrated a time- and concentration-dependent increase in HL-60 cell adherence to influenza virus-infected endothelial cell monolayers that is predominantly due to HA, the newly expressed surface viral protein. These findings indicate that viral proteins can directly enhance leukocyte binding to infected cells. The findings also suggest that the expression of viral proteins on virus-infected cells may be an important step in virally mediated endothelial injury and the subsequent development of inflammatory responses.

### Acknowledgments

We thank HMC Keith Brockgreitens for maintaining cell cultures and performing the adhesion and cytotoxicity assays. We would also like to thank Dr. Terry Pellmar, Dr. Gregory King, and Dr. Dan Goldman for critically reading the manuscript.

### References

1. Shasby, D. M., K. M. Vanbenthuyzen, R. M. Tate, S. S. Shasby, I. McMurtry, and J. E. Reprine. 1982. Granulocytes mediate acute edematous lung injury in rabbits and in isolated rabbit lungs perfused with phorbol myristate acetate: role of oxygen radicals. *Am. Rev. Respir. Dis.* 125:443.
2. Sacks, T., C. F. Moldow, P. R. Craddock, T. K. Bowers, and M. S. Jacob. 1978. Oxygen radicals mediate endothelial cell damage by complement-stimulated granulocytes: an in vitro model of immune vascular damage. *J. Clin. Invest.* 61:1161.
3. Harlan, J. M., P. D. Killen, L. A. Harker, and G. E. Striker. 1981. Neutrophil-mediated endothelial injury in vitro: mechanisms of cell detachment. *J. Clin. Invest.* 68:1394.
4. Ward, P. A., and J. Varani. 1990. Review: Mechanisms of neutrophil mediated killing of endothelial cells. *J. Leukocyte Biol.* 48:97.
5. Gocke, D. J., K. Hsu, C. Morgan, S. Bombardieri, M. Lockshin, and C. L. Christian. 1971. Vasculitis in association with Australia antigen. *J. Exp. Med.* 134:330s.
6. Zimmerman, G. A., A. D. Renzetti, and H. R. Hill. 1984. Granulocyte adherence in pulmonary and systemic arterial blood samples from patients with adult respiratory distress syndrome. *Am. Rev. Respir. Dis.* 129:798.
7. Visser, M. R., H. S. Jacob, J. L. Goodman, J. B. McCarthy, L. T. Furcht, and G. M. Vercellotti. 1989. Granulocyte-mediated injury to herpes simplex virus-infected human endothelium. *Lab. Invest.* 60:296.
8. Fabricant, C. G., J. Fabricant, M. M. Litrenta, and C. R. Minick. 1978. Virus-induced atherosclerosis. *J. Exp. Med.* 148:335.
9. Benditt, E. P., T. Barrett, and J. K. McDougall. 1983. Viruses in the etiology of atherosclerosis. *Proc. Natl. Acad. Sci. USA* 80:6386.
10. Gyorkey, F., J. L. Melnick, G. A. Guinn, P. Gyorkey, and M. E. DeBakey. 1984. Herpesviridae in the endothelial and smooth muscle cells of the proximal aorta in arteriosclerotic patients. *Exp. Mol. Pathol.* 40:328.
11. MacGregor, R. R., H. M. Friedman, E. J. Macarak, and N. A. Kefalides. 1980. Virus infection of endothelial cells increases granulocyte adherence. *J. Clin. Invest.* 65:1469.
12. Kirkpatrick, C. J., B. D. Bultmann, and H. Gruler. 1985. Interaction between enteroviruses and human endothelial cells in vitro: alterations in the physical properties of endothelial cell plasma membrane and adhesion of human granulocytes. *Am. J. Pathol.* 118:15.
13. Zajac, B. A., K. O'Neill, H. M. Friedman, and R. R. MacGregor. 1988. Increased adherence of human granulocytes to herpes simplex virus type 1 infected endothelial cells. *In Vitro Cell. & Dev. Biol.* 24:321.
14. Tuder, R. M., A. Weinberg, N. Panajotopoulos, and J. Kalil. 1991. Cytomegalovirus enhances PBMC binding and HLA class I expression on cultured endothelial cells. *Transplant. Proc.* 23:91.
15. Span, A. H., C. P. van Boven, and C. A. Bruggeman. 1989. The effect of cytomegalovirus infection on the adherence of polymorphonuclear leucocytes to endothelial cells. *Eur. J. Clin. Invest.* 19:542.
16. Span, A. H., J. Endert, C. P. van Boven, and C. A. Bruggeman. 1989. Virus induced adherence of monocytes to endothelial cells. *FEMS Microbiol. Immunol.* 1:237.
17. Span, A. H. M., M. C. E. van Dam-Mieras, W. Mullers, J. Endert, A. D. Muller, and C. A. Bruggeman. 1991. The effect of virus infection on the adherence of leukocytes or platelets to endothelial cells. *Eur. J. Clin. Invest.* 21:331.
18. Span, A. H. M., W. Mullers, A. M. M. Miltenburg, and C. A. Bruggeman. 1991. Cytomegalovirus induced PMN adherence in relation to an ELAM-1 antigen present on infected endothelial cell monolayers. *Immunology* 72:355.
19. Dustin, M. L., and T. A. Springer. 1988. Lymphocyte

- function-associated antigen-1 (LFA-1) is one of at least three mechanisms for lymphocyte adhesion to cultured endothelial cells. *J. Cell Biol.* 107:321.
20. Diamond, M. S., D. E. Staunton, A. R. de Fougerolles, S. A. Stackner, J. Garcia-Aguilar, M. L. Hibbs, and T. A. Springer. 1990. ICAM-1 (CD54): a counter-receptor for Mac-1 (CD11b/CD18). *J. Cell Biol.* 111:3129.
  21. Smith, C. W. 1990. Molecular determinants of neutrophil adhesion. *Am. J. Respir. Cell Mol. Biol.* 2:487.
  22. Jutila, M. A. 1992. Leukocyte traffic to sites of inflammation: review article. *APMIS.* 100:191.
  23. Polley, M. J., M. L. Phillips, E. Wayner, E. Nudelman, A. K. Singhal, S. Hakomori, and J. C. Paulson. 1991. CD62 and endothelial cell-leukocyte adhesion molecule 1 (ELAM-1) recognize the same carbohydrate ligand, sialyl-Lewis x. *Proc. Natl. Acad. Sci. USA* 88:6224.
  24. Picker, L. J., R. A. Warnock, A. R. Burns, C. M. Doerschuk, E. L. Berg, and E. C. Butcher. 1991. The neutrophil selectin LECAM-1 presents carbohydrate ligands to the vascular selectins ELAM-1 and GMP-140. *Cell* 66:921.
  25. Etingin, O. R., R. L. Silverstein, and D. P. Hajjar. 1991. Identification of a monocyte receptor on herpesvirus-infected endothelial cells. *Proc. Natl. Acad. Sci. USA* 88:7200.
  26. Colden-Stanfield, M., D. Ratcliffe, E. Cramer, and E. Gallin. 1992. Mechanism(s) of enhanced human promyelocytic leukemia cell (HL60) adherence to influenza virus (WSN)-infected endothelium. *FASEB J.* 6:A1888.
  27. Stanley, E. D., and G. G. Jackson. 1966. Viremia in Asian influenza. *Trans. Assoc. Am. Physicians* 79:376.
  28. Khakpour, M., A. Sardi, and K. Naficy. 1969. Proved viraemia in Asian influenza (Hong Kong variant) during incubation period. *Br. Med. J.* 4:208.
  29. Kaji, M., R. Oseasohn, W. S. Jordan, Jr., and J. M. Dingle. 1958. Isolation of Asian virus from extrapulmonary tissues in fatal human influenza. *Proc. Soc. Exp. Biol. Med.* 100:272.
  30. Lehmann, N. I., and I. D. Gust. 1971. Viremia in influenza: a report of two cases. *Med. J. Aust.* 2:1166.
  31. Roberts, G. T., and J. T. Roberts. 1976. Postsplenectomy sepsis due to influenzal viremia and pneumococemia. *Can. Med. Assoc. J.* 115:435.
  32. Ray, C. G., T. B. Icenogle, L. L. Minnich, J. G. Copeland, and T. M. Grogan. 1989. The use of intravenous ribavirin to treat influenza virus-associated acute myocarditis. *J. Infect. Dis.* 159:829.
  33. Jaffe, E. A., R. L. Nachman, C. G. Becker, and C. R. Minick. 1973. Culture of human endothelial cells derived from umbilical veins: identification by morphologic and immunologic criteria. *J. Clin. Invest.* 52:2745.
  34. Gimbrone, M. A., Jr. 1976. Culture of vascular endothelium. *Prog. Hemostasis Thromb.* 3:1.
  35. Voyta, J. C., D. P. Via, C. E. Butterfield, and B. R. Zetter. 1984. Identification and isolation of endothelial cells based on their increased uptake of acetylated-low density lipoprotein. *J. Cell Biol.* 99:2034.
  36. Rodriguez-Boulan, E. 1983. Polarized assembly of enveloped viruses from cultured epithelial cells. *Methods Enzymol.* 98:486.
  37. Kuchler, R. J. 1977. Isolation and identification of animal viruses. In *Biochemical Methods in Cell Culture and Virology*. Dowden, Hutchinson & Ross, Inc., Stroudsburg, PA, p. 144.
  38. Malherbe, N. H. 1985. Role of tissue culture systems. In *Laboratory Diagnosis of Viral Infections*. E. H. Lennette, ed. Marcel Dekker, Inc., New York, NY, p. 4753.
  39. Ratcliffe, D. R., S. L. Nolin, and E. B. Cramer. 1988. Neutrophil interaction with influenza-infected epithelial cells. *Blood* 72:142.
  40. Reed, L. J., and J. Muench. 1938. A simple method of estimating fifty per cent endpoints. *Am. J. Hyg.* 27:493.
  41. Pohlman, T. H., K. A. Stanness, P. G. Beatty, H. D. Ochs, and J. M. Harlan. 1986. An endothelial cell surface factor(s) induced in vitro by lipopolysaccharide, interleukin 1, and tumor necrosis factor- $\alpha$  increases neutrophil adherence by a CDw-18-dependent mechanism. *J. Immunol.* 136:4548.
  42. Schleimer, R. P., and B. K. Rutledge. 1986. Cultured human vascular endothelial cells acquire adhesiveness for neutrophils after stimulation with interleukin 1, endotoxin, and tumor-promoting phorbol diesters. *J. Immunol.* 136:649.
  43. Bevilacqua, M. P., J. S. Pober, D. L. Mendrick, R. S. Cotran, and M. A. Gimbrone. 1987. Identification of an inducible endothelial-leukocyte adhesion molecule. *Proc. Natl. Acad. Sci. USA* 84:9238.
  44. Smith, C. W., R. Rothlein, B. J. Hughes, M. M. Mariscalco, H. E. Rudloff, F. C. Schmalstieg, and D. C. Anderson. 1988. Recognition of an endothelial determinant for CD18-dependent human neutrophil adherence and transendothelial migration. *J. Clin. Invest.* 82:1746.
  45. Lazarowitz, S. G., R. W. Campano, and P. W. Choppin. 1971. Influenza virus structural and nonstructural proteins in infected cells and their plasma membranes. *Virology* 46:830.
  46. Pahwa, S., D. Kirkpatrick, C. Ching, C. Lopez, R. Pahwa, E. Smithwick, R. O'Reilly, C. August, P. Pasquariello, and R. A. Good. 1983. Persistent cytomegalovirus infection: association with profound immunodeficiency and treatment with interferon. *Clin. Immunol. Immunopathol.* 28:77.
  47. Dolin, R., D. D. Richman, B. R. Murphy, and A. S. Fauci. 1977. Cell mediated immune responses in humans after induced infection with influenza A virus. *J. Infect. Dis.* 135:714.
  48. Criswell, B. S., R. B. Couch, S. B. Greenberg, and S. L. Kimzey. 1979. The lymphocyte response to influenza in humans. *Am. Rev. Respir. Dis.* 120:700.
  49. Fischer, J. J., and D. H. Walker. 1979. Invasive pulmonary aspergillosis associated with influenza. *JAMA* 241:1493.
  50. Schooley, R. T., P. Densen, D. Harmon, D. Felsenstein, M. S. Hirsch, W. Henle, and S. Weitzman. 1984. Antineutrophil antibodies in infectious mononucleosis. *Am. J. Med.* 76:85.
  51. Friedman, H. M., E. J. Macarak, R. R. MacGregor, J. Wolfe, and N. A. Kefalides. 1981. Virus infection of endothelial cells. *J. Infect. Dis.* 143:266.
  52. Colden-Stanfield, M., E. B. Cramer, and E. K. Gallin. 1992. Comparison of apical and basal surfaces of confluent endothelial cells: patch-clamp and viral studies. *Am. J. Physiol.* 263 (Cell Physiol. 32):C573.
  53. Bevilacqua, M. P., J. S. Pober, M. E. Wheeler, D. Mendrick, R. S. Cotran, and M. A. Gimbrone, Jr. 1985. Interleukin-1 (IL-1) acts on vascular endothelial cells to increase their adhesiveness for blood leukocytes. *J. Clin. Invest.* 76:2003.
  54. Cavender, D. E., D. O. Haskard, B. Joseph, and M. Ziff. 1986. Interleukin 1 increases the binding of human B and T lymphocytes to endothelial cell monolayers. *J. Immunol.* 136:203.
  55. Dustin, M. L., R. Rothlein, A. K. Bhan, C. A. Dinarello, and

- T. M. Springer. 1986. Induction by IL-1 and interferon- $\gamma$ : Tissue distribution, biochemistry, and function of a natural adherence molecule (ICAM-1). *J. Immunol.* 137:245.
56. Miller, L. J., R. Schwartig, and T. M. Springer. 1986. Regulated expression of the Mac-1, LFA-1, P150,95 glycoprotein family during leukocyte differentiation. *J. Immunol.* 137:2891.
57. Back, A. L., K. A. Gollahon, and D. D. Hickstein. 1992. Regulation of expression of the leukocyte integrin CD11a (LFA-1) molecule during differentiation of HL-60 cells along the monocyte/macrophage pathway. *J. Immunol.* 148:710.
58. Tosi, M. F., J. M. Stark, A. Hamedani, C. W. Smith, D. C. Gruenert, and Y. T. Huang. 1992. Intercellular adhesion molecule-1 (ICAM-1)-dependent and ICAM-1-independent adhesive interactions between polymorphonuclear leukocytes and human airway epithelial cells infected with parainfluenza virus type 2. *J. Immunol.* 149:3345.
59. Patel, K. D., G. A. Zimmerman, S. M. Prescott, R. P. McEver, and T. M. McIntyre. 1991. Oxygen radicals induce human endothelial cells to express GMP-140 and bind neutrophils. *J. Cell Biol.* 112:749.
60. Ratcliffe, D., J. Michl, and E. Cramer. 1989. Neutrophils and monocytes adhere to influenza-infected epithelia via viral haemagglutinin molecules. *J. Cell Biol.* 107(6):554a.
61. Ratcliffe, D., G. Migliorisi, and E. Cramer. 1992. Translocation of influenza virus by migrating neutrophils. *Cell. Mol. Biol.* 38:63.
62. Naficy, K. 1963. Human influenza infection with proved viremia: report of a case. *N. Eng. J. Med.* 269:964.
63. Lawrence, M. B., and T. A. Springer. 1991. Leukocytes roll on a selectin at physiologic flow rates: distinction from and prerequisite for adhesion through integrins. *Cell* 65:859.
64. Sastry, M. V. K., M. J. Swamy, and A. Surolia. 1988. Analysis of dynamics and mechanism of ligand binding to Artocarpus integrifolia agglutinin. *J. Biol. Chem.* 263:14826.
65. Chakrabarti, A., and S. K. Podder. 1990. Complex carbohydrate-lectin interaction at the interface: a model for cellular adhesion. I. Effect of vesicle size on the kinetics of aggregation between a fatty acid conjugate of lectin and a liposomal asialoganglioside. *Biochim. Biophys. Acta* 1024:103.
66. Gupta, D., N. V. S. Prasad Rao, K. D. Puri, K. L. Matta, and A. Surolia. 1992. Thermodynamic and kinetic studies on the mechanism of binding of methylumbelliferyl glycosides to jacalin. *J. Biol. Chem.* 267:8909.
67. Duzgunes, N. M. C. Pedroso de Lima, L. Stamatatos, D. Flasher, D. Alford, D. S. Friend, and S. Nir. 1992. Fusion activity and inactivation of influenza virus: kinetics of low pH-induced fusion with cultured cells. *J. Gen. Virol.* 73:27.
68. Sauter, N. K., M. D. Bednarski, B. A. Wurzburg, J. E. Hanson, G. M. Whitesides, J. J. Skehel, and D. C. Wiley. 1989. Haemagglutinins from two influenza virus variants bind to sialic acid derivatives with millimolar dissociation constants: a 500-MHz proton nuclear magnetic resonance study. *Biochemistry* 28:8388.
69. Hanson, J. E., N. K. Sauter, J. J. Skehel, and D. C. Wiley. 1992. Proton nuclear magnetic resonance studies of the binding of sialosides to intact influenza virus. *Virology* 189:525.



# Antibodies Chaperone Circulating IL-6

## Paradoxical Effects of Anti-IL-6 "Neutralizing" Antibodies in Vivo<sup>1</sup>

Lester T. May,\* Ruth Neta,<sup>†</sup> Lyle L. Moldawer,<sup>‡</sup> John S. Kenney,<sup>§</sup> Kirit Patel,\* and Pravin B. Sehgal<sup>2,\*†</sup>

\*Department of Microbiology and Immunology, and <sup>†</sup>Medicine, New York Medical College, Valhalla, NY 10595; <sup>‡</sup>Armed Forces Radiobiology Research Institute, Bethesda, MD 20814; <sup>§</sup>Department of Surgery, Cornell University Medical College, New York, NY 10021; <sup>§</sup>Department of Inflammation Biology and Immunology, Syntex Research, Palo Alto, CA 94304

**ABSTRACT.** In the baboon or the mouse, a stimulus such as LPS, TNF, or IL-1 typically led to a rapid induction of circulating IL-6, the levels peaked by 2 to 3 h and then declined to near-baseline values by 6 to 8 h. Administration to baboons or mice of "neutralizing" anti-IL-6 mAb followed by an IL-6 inducer led to a marked and sustained increase in circulating IL-6 levels. IL-6 Ag, IL-6 biologic activity, neutralizing anti-IL-6 mAb, and IL-6/anti-IL-6 mAb complexes could all be observed for an extended period of time (beyond 8 h) in the circulation of such animals. Nevertheless, in mice, if the anti-IL-6 mAb had been administered before the IL-6 inducer, there was a reduction in the *in vivo* IL-6-induced stimulation of fibrinogen levels, indicating that most of the intravascular IL-6 was not readily available for eliciting hepatocyte effects under these experimental conditions. Intraperitoneal administration into mice of mixtures of murine rIL-6 or human rIL-6 together with their respective anti-IL-6 mAb led to a marked increase in the appearance and longevity in the peripheral circulation of the exogenously administered murine or human rIL-6 species in a biologically active form. Varying the ratio of human rIL-6 to anti-human IL-6 mAb indicated that a molar ratio of 1:1 was sufficient for the ability of mAb to chaperone IL-6 in the murine circulation. Human rIL-6 mixed with "neutralizing" mAb in the approximate ratio 1:1 elicited an enhanced fibrinogen response *in vivo* in the mouse; an IL-6:mAb ratio of 1:125 led to a reduction in the fibrinogen response even though the levels of circulating B9 bioactivity and of human rIL-6-Ag were maximal under these conditions. Gel-filtration chromatographic and Western blotting analyses of IL-6 present *in vivo* in the mAb-free baboon revealed that although the IL-6 Ag was largely present in high molecular mass complexes of size 400 kDa in association with soluble IL-6 receptor, the B9 bioactivity was largely of low molecular mass (20 kDa). In contrast, in the anti-IL-6 mAb-treated baboon or mouse, the IL-6 Ag and bioactivity were both largely in complexes of mass 200 kDa. Thus, the binding of IL-6 in the intravascular compartment to other proteins, anti-IL-6 mAb in the present studies, gives IL-6 unexpected biochemical and pharmacologic properties *in vivo*. *Journal of Immunology*, 1993, 151: 3225.

**P**assive immunization of experimental animals with neutralizing antibodies to various cytokines or with blocking antibodies to cytokine receptors has proven to be a powerful approach to evaluate the contribution of specific cytokines to host defense (1-7). The functional deletion of a particular cytokine such as TNF, IL-1, or IFN can either exacerbate or ameliorate the course of particular infections depending on the animal model and the

infecting organism studied. This approach has provided evidence for a protective role of IFN- $\alpha/\beta$  in various acute viral infections (8, 9), an exacerbating role of IFN- $\alpha/\beta$  in lymphocytic choriomeningitis virus infections (10), a del-

Received for publication February 5, 1993. Accepted for publication June 16, 1993.

The costs of publication of this article were defrayed in part by the payment of page charges. This article must therefore be hereby marked advertisement in accordance with 18 U.S.C. Section 1734 solely to indicate this fact.

<sup>1</sup> This work was supported in part by Research Grants AI-16262 (P.B.S.), GM-40586 (L.L.M.), Grant-in-Aid 92-363GS (L.T.M.) from the American Heart Association New York state affiliate, a contract from the National Foundation for Cancer Research, the Armed Forces Radiobiology Research Institute, Defense Nuclear Agency, work unit 00129, and a grant from Toray Industries, Japan. Views presented in this paper are those of the authors; no endorsement by the Defense Nuclear Agency or the Department of Defense has been given or should be inferred.

<sup>2</sup> Address correspondence and reprint requests to Dr. P. B. Sehgal, Department Microbiology and Immunology, Basic Science Building, New York Medical College, Valhalla, NY 10595.

eterious effect of TNF and IL-1 in gram-negative sepsis (2, 3), and a protective role of TNF and IL-1 in gram-positive *Listeria sepsis* (4, 5). With the recognition of IL-6 as the major systemic cytokine that mediates the acute phase response (11, 12), which includes the alterations in hepatic plasma protein synthesis in response to various infections and other tissue injury, and the availability of potent "neutralizing" mAb to human and murine rIL-6 (13-15), attempts have been made to evaluate the role of endogenous IL-6 in host defense using the passive immunization approach (14, 16). However, in contrast to the experience with other cytokines (1-7), we (17) and others (18, 19) have observed that, paradoxically, passive immunization with neutralizing anti-IL-6 mAb resulted in even higher levels of biologically active IL-6 in the peripheral circulation even though, in at least some instances, anti-IL-6 mAb blocked endogenous IL-6-mediated effects (16, 20). What is the biochemical basis for this dissociation? Why is circulating IL-6 not always bioavailable in vivo?

In previous studies we have shown that IL-6 can exist in human plasma or serum at high concentrations (in the ng/ml to  $\mu\text{g/ml}$  range) in complexes of size 100 to 150 and 400 to 500 kDa that, in addition to the soluble IL-6 receptor, contain cleavage fragments from C-reactive protein, and complement C3 and C4 (13). When present in such complexes, the natural human IL-6 molecule is essentially camouflaged, displays little B9 hybridoma proliferation bioactivity and is not accessible using ELISA that otherwise are very sensitive to rIL-6. Indeed, it was the development of an ELISA that preferentially detected human IL-6 in such high molecular mass complexes (13) that suggested that IL-6 does not customarily exist as a free cytokine in the human circulation and led us to ask the question: what is the biologic activity of IL-6 as it exists in vivo?

Baboons challenged with a bolus of *Escherichia coli* or of endotoxin have been used as a useful model to investigate the cytokine, hemodynamic, and other physiologic events that underlie acute Gram-negative sepsis (1). Passive immunization with anti-TNF mAb or with anti-IL-1 receptor antagonist in this model reduced the observed morbidity indicating that TNF and IL-1 produced during acute Gram-negative sepsis were deleterious to the host (1-3, 7, 21). In light of the induction of IL-6 in this model, as an event secondary to TNF and IL-1 synthesis (2, 21), we examined the effect of passive immunization with the anti-HuIL-6 mAb "5IL6-H17" in the LPS-treated baboon. Passive immunization studies were also initiated using the anti-MuIL-6 mAb "20F3-MP5" (22) in LPS-, TNF-, or IL-1-treated mice. We report that anti-IL-6 mAb, even though they "neutralized" rIL-6 activity in cell-culture experiments, exerted a chaperoning effect on endogenously produced or exogenously administered IL-6 in vivo. The data obtained highlight a novel aspect of IL-6 biology—IL-6 can circulate in vivo as part of a protein aggregate and in this state its biologic function is markedly altered.

## Materials and Methods

### Experimental animals

CD2F1 female mice were purchased from the Animal Genetics and Production Branch, National Cancer Institute, National Institutes of Health (Frederick, MD). Mice were handled as previously described (6, 20); each experimental group consisted of two to four animals per variable per time point. All animals in each group were killed at each time point. For fibrinogen assays, sera from individual animals were assayed separately; sera from all animals in a particular group were pooled before assays for IL-6 (B9 bioassay, hepatocyte bioassay, or ELISA). Each experiment was replicated at least three times.

Two young adult baboons (*Papio sp.*) weighing 26 (baboon 90-11) and 22 (baboon 90-12) kg were used (21). Baboons were obtained from the National Primate Exchange through Buckshire Laboratories (Chelmsford, PA). Animals were quarantined at the Research Animal Resource Center of Cornell University Medical College for 2 to 4 wk before study to confirm that they were in good health and free of transmissible diseases. Baboons were fasted overnight and anesthetized with intramuscular ketamine hydrochloride (10 mg/kg). The animals were instrumented for invasive hemodynamic monitoring as previously described (21). Both animals received the i.v. administration of 500  $\mu\text{g/kg}$  of *Salmonella typhosa* LPS. One of the animals (baboon 90-12) received 2.15 mg/kg of an anti-Hu<sup>3</sup>IL-6 mAb (5IL6-H17) 2 h before the LPS (purchased from Sigma Chemical Co., St. Louis, MO) injection. Hemodynamic parameters and urine output were monitored continuously. Arterial blood was collected at 30-min intervals for the first 3 h, and at hourly intervals thereafter for 8 h. At the end of the 8 h period, the baboons were allowed to awaken and were returned to their cages.

### B9 growth factor assay for IL-6

The IL-6 content of the various preparations were assayed by monitoring their ability to induce the proliferation of murine B9 hybridoma cells using standardized procedures described earlier (23, 24). The interim reference standard for IL-6 88/514 was included in every assay.

### Hepatocyte-stimulating factor assay for murine IL-6

The rat hepatoma line H4-II-E-C3 that was derived by subcloning the Reuber H-35 rat hepatoma line was purchased from the American Type Culture Collection (Rockville, MD, ATCC CRL 1600) and grown to 80 to 90% confluency in Falcon T-75 flasks in Eagle's MEM with 10% (v/v) heat-inactivated FCS (GIBCO, Grand Island, NY), 0.1 mM sodium pyruvate and "MEM nonessential amino acids"

<sup>3</sup> Abbreviations used in this paper: Hu, human; Ab, antibody; Mu, murine; V<sub>e</sub>, excluded volume; V<sub>i</sub>, included volume; V<sub>o</sub>, void volume; sIL-6R, soluble IL-6 receptor.

(GIBCO). The cells were then passaged and placed in 24-well Falcon tissue culture plates with  $1 \times 10^5$  cells per well of growth medium. After 24 h the medium was changed to serum-free growth medium supplemented with  $1 \mu\text{M}$  dexamethasone and various dilutions of samples to be tested for hepatocyte-stimulating activity. After incubation for 24 h the cultures were washed with PBS and incubated for an additional 24 h in methionine-free medium containing  $^{35}\text{S}$ -methionine ( $100 \mu\text{Ci/ml}$ ). The culture medium from each well was then collected and the amount of  $^{35}\text{S}$ -methionine-labeled fibrinogen secreted was quantitated by immunoprecipitation (goat antiserum to rat fibrinogen was purchased from Cappel, Durham, N. Carolina), SDS-PAGE (12%), autoradiography, and densitometry using procedures similar to those described previously (25). Laboratory standards for IL-6 were derived from baculovirus-derived recombinant murine IL-6 that were estimated to be  $>95\%$  pure by Coomassie-stained SDS-PAGE and whose sp. act. was  $1$  to  $2 \times 10^9$  B9 U/mg of IL-6 protein (24).

#### ELISA for baboon IL-6

ELISAs were formatted and performed essentially as described by Kenney et al. (26). Several different anti-HuIL-6 two mAb sandwich ELISA (IG61/SIL6, 4IL6/SIL6 and 7IL6/SIL6) (13) were used that have been previously evaluated using different preparations of natural human IL-6 as well as with rHuIL-6 produced using different vector systems (13, 24). Human *E. coli*-derived rIL-6 reference preparation 88/514 was used to calibrate every assay.

#### Sephadex G-200 gel filtration chromatography

Serum or fresh plasma samples (0.5–1.2 ml) were fractionated through a Sephadex G-200 column ( $2.5 \times 60$  cm;  $V_0 = 55$  ml;  $V_e = 164$  ml;  $V_i = V_e - V_0$ ). Eluate fractions of volume 2.5 ml were collected after the first  $V_0$  and continued for an additional two  $V_0$  (approximately 50 fractions) (13). All eluted fractions were calibrated by size through the use of the following marker proteins: ribonuclease-13.7 kDa; chymotrypsinogen A-43 kDa; OVA-67 kDa; aldolase-158 kDa; catalase-232 kDa; and ferritin-440 kDa. The Sephadex G-200 and the calibrating proteins were purchased from Pharmacia LKB (Picataway, NJ).

#### SDS-PAGE and Western blot analysis

Aliquots of various baboon IL-6 preparations were concentrated by lyophilization and resuspended in Laemmli buffer (27), heated for 1 to 2 min at  $100^\circ\text{C}$ , subjected to SDS-PAGE under reducing conditions (0.7 M  $\beta$ -mercaptoethanol) and transferred to WESTRAN polyvinylidene difluoride membranes (Schleicher & Schuell, Keene, NH) according to the method of Towbin et al. (28). The baboon IL-6 or sIL-6R species on the electroblotted polyvinylidene difluoride membrane were detected using, respectively, a

rabbit polyclonal antibody raised to rHuIL-6 (29) or an anti-IL-6R mAb (MT-18) (30) and an immunoperoxidase procedure (Vectastain, ABC Elite kit, Burlingame, CA).

#### Immunoaffinity purification of IL-6 from mouse or baboon plasma

In order to further purify and concentrate IL-6 from G-200 gel chromatography fractions of plasma from the variously treated mice or baboons, immunoaffinity columns were prepared with either mAb to murine IL-6 (mAb 20F3-MP5) or HuIL-6 (mAb 5IL6-H17) as previously described (13). Sephadex G-200 fractions were pooled around peaks in IL-6 ELISA or B9 growth factor activities. These pools were then passed through a 1- to 2-cm column of either 5IL6- or 20F3-mAb affinity resin and the adsorbed IL-6 extensively washed with 150 mM NaCl, 10 mM Tris-Cl, pH 7.5. The adsorbed IL-6 was eluted upon addition of 0.1 M glycine, pH 2.4, and the eluted fractions were immediately neutralized with equimolar amounts of Tris-Cl, pH 8.7.

#### Immunoaffinity purification of sIL-6R from baboon plasma

To purify sIL-6R species present in high molecular mass complexes in baboon plasma, pools of appropriate Sephadex G-200 gel filtration fractions representing 200 to 400 kDa were passed through a 1- to 2-cm immunoaffinity column containing the anti-HuIL-6R mAb MT-18 (30) covalently bound to the affinity resin (13). The adsorbed sIL-6R species were eluted upon addition of 0.1 M glycine, pH 2.4, and the eluted fractions were immediately neutralized with equimolar amounts of Tris-Cl, pH 8.7.

#### Fibrinogen assay of murine plasma

Fibrinogen in citrated plasma was measured as the rate of conversion of fibrinogen to fibrin in the presence of excess thrombin using the Sigma Diagnostic kit (Sigma) for calibration (6, 20). The data are expressed as mg of fibrinogen per 100 ml of plasma. Measurement of fibrin clot formation were performed using a fibrometer (Becton Dickinson, Fairleigh, NJ).

#### Other materials and procedures

Rat mAb to mouse rIL-6 (MP5 20F3) was prepared using semipurified Cos-7 mouse IL-6 as an immunogen, as previously described (21). An isotype-matched control rat mAb to  $\beta$ -galactosidase (GL113) was used (20, 21). rHuIL-1 $\alpha$  (lot IL-1 2/88; sp. act.  $3 \times 10^8$  U/mg) was kindly provided by Dr. Peter Lomedico (Hoffmann-La Roche, Inc., Nutley, NJ). Murine rTNF- $\alpha$  (lot 4296-17; sp. act.  $2 \times 10^4$  U/mg as assayed on L929 cells) was kindly provided by Dr. Grace Wong (Genentech Inc., South San Francisco, CA). An additional preparation of rHuIL-6 (SDZ 280-969; sp. act.  $52 \times 10^6$  U/mg by B13.29 assay) was also obtained

from E. Liehl, Sandoz Forschungsinstitut (Vienna, Austria) and of murine rIL-6 ( $ED_{50}$  in B9 bioassay of 0.2 ng/ml) from Pepro-Tech Inc. (Rocky Hill, NJ). All cytokine and mAb preparations used were free of endotoxin as assayed using the chromogenic limulus amoebocyte lysate kit (Whittaker, Walkersville, CA).

In the murine experiments the antibodies and recombinant cytokines were diluted in pyrogen-free saline on the day of the injection and were administered i.p. Typically antibodies were administered to mice i.p. 6 to 20 h before i.p. injection of cytokines (20).

#### Statistical analyses

Between group comparisons were carried out using the Student's *t*-test and ANOVA procedures (True Epistat, Richardson, TX).

### Results

#### Anti-HuIL-6 mAb in LPS-treated baboon

The murine mAb "5IL6-H17" prepared against rHuIL-6 (13) effectively neutralized IL-6 present in LPS-induced

baboon plasma as assayed in the B9 bioassay (data not shown). Therefore, this anti-HuIL-6 mAb was used for passive immunization in the endotoxin-treated baboon. Baboon 90-12 was given anti-HuIL-6 mAb at a dose of 2.1 mg/kg body weight followed 8 h later with an i.v. challenge with *S. typhosa* LPS (500  $\mu$ g/kg body weight). It had been determined from previous experiments that this dose of LPS led to significant morbidity (alterations in hemodynamics and body temperature) (2, 3, 21). Furthermore, this LPS dose was confirmed by us to lead to plasma IL-6 induction by 1 to 2 h, a peak level by 3 to 4 h and a decline to base-line levels by 6 to 8 h (data not shown). Importantly, the IL-6 levels were assayable using both the B9 bioassay and the 4IL6/5IL6 ELISA (see control baboon 90-11 in Fig. 1, A and B). In comparison to the control baboon 90-11, the 4IL6/5IL6 ELISA showed that very little apparent IL-6 was present in the mAb-treated animal, simultaneously with the presence of high levels of circulating anti-HuIL-6 mAb (5IL6-H17) (Fig. 1, B and C) and of baboon IL-6/anti-HuIL-6 mAb complexes (Fig. 1D). When serial threefold dilutions of plasma from baboon 90-12 were first assayed

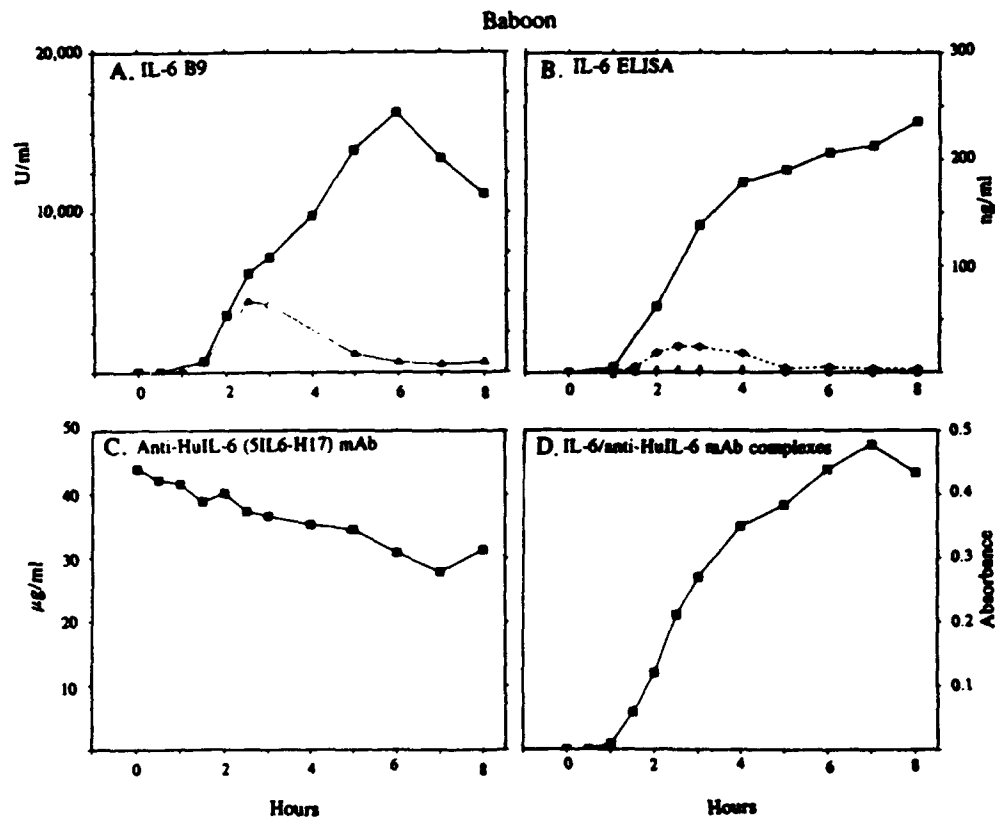
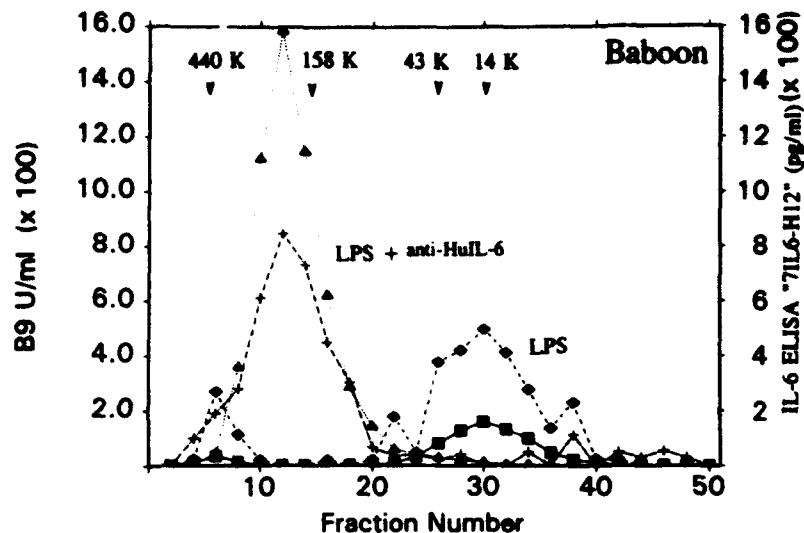


**FIGURE 1.** Circulating IL-6, anti-HuIL-6 mAb (5IL6-H17) and IL-6/anti-HuIL-6 mAb complexes in LPS-treated baboons. Baboon 90-11 was administered LPS at time "0," baboon 90-12 was administered anti-HuIL-6 mAb 5IL6-H17 2 h before the LPS challenge. A, Plasma IL-6 levels as measured in the B9 bioassay in baboons 90-11 (○) and 90-12 (■). B, Plasma IL-6 levels as measured in the 4IL6/5IL6 ELISA in baboons 90-11 (◆) and 90-12 (◊). Also plasma IL-6 levels as measured in the IG61/5IL-6 ELISA in baboon 90-12 (■). C, Plasma levels of the murine anti-HuIL-6 mAb 5IL6-H17 in baboon 90-12 (■) as measured in an anti-murine-Ig immunoassay. D, Plasma levels of IL-6/anti-HuIL-6 mAb complexes in baboon 90-12 (■) as measured using the anti-murine-Ig Ab (goat) as the capture reagent and biotinylated 4IL6-H11 mAb as the developing reagent (the goat anti-mouse-Ig captures 5IL6-H17 mAb; the ELISA plate is then flooded with mouse Ig, and the biotinylated 4IL6-H11 then reports on baboon IL-6 bound to the captured 5IL6-H17 mAb).

**FIGURE 2.** Sephadex G-200 gel filtration analyses of IL-6 present in baboon plasma. Aliquots (1 ml) of plasma from baboons 90-11 (2.5-h time point) and 90-12 (8-h time point) were fractionated through a G-200 gel filtration column. IL-6 bioactivity present in the eluted fractions was assayed in the B9 bioassay (90-11, ■; 90-12, ○). IL-6 Ag present in eluted fractions was assayed in the 7IL6/5IL6 ELISA (90-11, ◆; 90-12, +).



for B9 activity starting with an initial dilution of 1:20, little biologic activity was observed. However, repeating the assays with the baboon 90-12 plasma samples diluted beyond approximately 1/500 uncovered high titers of B9 bioactivity in this anti-IL-6 mAb-treated animal (Fig. 1A). On repeating the IL-6 ELISA using a different high-affinity capture antibody (mAb "IG61") high levels of IL-6 Ag (up to and exceeding 200 ng/ml) were readily observed in the mAb-treated baboon (Fig. 1B). The data indicate that the selection of mAbs to be used in the ELISA assay is critical and may lead to disparate results. Furthermore, unless B9-biologic activity is adequately assayed for across an extensive dilution series, the paradoxical enhancement in circulating IL-6 levels produced by "neutralizing" anti-IL-6 mAb can be overlooked.

The anti-HuIL-6 mAb present in baboon plasma retained the ability to neutralize exogenously added human or baboon IL-6 at least when assayed *ex vivo* in the B9 bioassay; the neutralization titers were in the range 3000 to 5000 neutralizing units/ml of baboon plasma (vs 10 U/ml baboon IL-6; data not shown). Furthermore, the B9 bioactivity present in both baboons 90-11 and 90-12 could be, in turn, completely neutralized *ex vivo* by addition of more anti-HuIL-6 mAb 5IL6-H17 or of a polyclonal rabbit anti-HuIL-6 antiserum (data not shown). Thus, the overall picture that emerged was that at one and the same time the circulation of the anti-IL-6 mAb- and LPS-treated baboon contained potent neutralizing anti-IL-6 mAb, high levels of IL-6 Ag (up to 0.20  $\mu\text{g}/\text{ml}$ ), biologically active IL-6 (at least as assayed *ex vivo*), and IL-6/anti-IL-6 mAb complexes.

#### High molecular mass IL-6 complexes in baboon with discrepant ELISA and B9 bioassay properties

IL-6 in sera from baboons 90-11 (mAb-free) and 90-12 (mAb-treated) was characterized biochemically. Aliquots (1 ml) of serum with highest IL-6 titer from each (the 2.5

h time point for baboon 90-11 and the 8 h time-point for baboon 90-12; see Fig. 1, A and B) were subjected to gel-filtration chromatography through a Sephadex G-200 column. The eluted fractions were assayed (1) in the B9 bioassay and (2) in the 7IL6/5IL6 ELISA.

Figure 2 shows that the major peak of B9 activity in baboon 90-11 was of molecular mass 15-25 kDa; a second small but reproducible peak was detected in fraction 6 corresponding to molecular mass of 400 kDa. The 7IL6/5IL6 ELISA data were consistent with these B9 bioassay results—a major peak at about 20 kDa and a minor peak at about 400 kDa were observed.

In contrast, the mAb-treated baboon 90-12, revealed a single major peak of B9 and ELISA reactivity of mass approximately 200 kDa. A trail of B9 bioactivity was detected extending to the lower molecular mass material suggesting the presence of an equilibrium state between the mAb and the IL-6. It was noteworthy that the relative ELISA to B9 ratio of the 200-kDa peak from baboon 90-12 (mAb-treated) was markedly lower than the same ratio for the 20-kDa IL-6 from baboon 90-11 (mAb-free). It is possible that the anti-HuIL-6 mAb present in the 200-kDa complex interfered with the ELISA or that the 200-kDa IL-6 complexes have novel binding properties (also see Table I).

To unambiguously determine why the relative ratios of ELISA signal to B9 activity varied for different forms of baboon IL-6, we purified the baboon IL-6 species in different G-200 filtration eluates. Pools of appropriate G-200 fractions were subjected to immunoaffinity column chromatography through an anti-HuIL-6-mAb (5IL6-H17) column (Table I). In each instance, the initial pool, the flow-through and the first two of the bound and eluted fractions (eluate 1 and eluate 2) were assayed in 1) B9 bioassay, 2) 7IL6/5IL6 ELISA, and 3) Western blot analysis. Only the first two eluted fractions (1 ml each) from each chromatography run had any B9 activity or ELISA reactivity.

**Table 1**  
Immunoaffinity chromatography through an mAb (5IL6-H17) column of baboon IL-6 present in pools of fractions derived from Sephadex G200 gel chromatography in Figure 2

Sample	IL-6		
	B9 U/ml	ELISA pg/ml (7IL6/5IL6)	Western blot*
<b>90-11, #3-14 (200-400 K)</b>			
Pool (load)	8	56	++
Flow-through	8	21	++++
Eluate 1	4	17	-
Eluate 2	3	17	-
<b>90-11, #27-37 (15-25 K)</b>			
Pool (load)	30	279	-
Flow-through	2	<16	-
Eluate 1	78	231	-
Eluate 2	103	816	+
<b>90-12, #3-7 (300-400 K)</b>			
Pool (load)	27	15	-
Flow-through	18	<15	++
Eluate 1	39	122	-
Eluate 2	21	48	-
<b>90-12, #8-14 (150-300 K)</b>			
Pool (load)	518	783	++
Flow-through	260	594	++++
Eluate 1	11	<10	-
Eluate 2	5	<10	-
<b>90-12, #27-37 (15-25 K)</b>			
Pool (load)	9	<10	-
Flow-through	6	<10	-
Eluate 1	<2	<10	-
Eluate 2	<2	<10	-

\* (-) absence of or (+) presence of detectable IL-6 species by SDS-PAGE and Western blotting using a rabbit anti-HuIL-6 antiserum. The volumes of the pool (load) were 9 ml, the flow-throughs were 9 ml and each eluate fraction was 1 ml.

The immunoaffinity column elution data show that IL-6 from baboons 90-11 and 90-12 had different mAb-reactivity characteristics (Table I). Most of the IL-6 from baboon 90-11 bound to and eluted from the anti-HuIL-6 mAb column (e.g., 90-11, 27-37, 15-25 kDa). In contrast, the IL-6 in baboon 90-12 failed to bind the anti-HuIL-6 mAb column (e.g., 90-12, 8-14, 150-300 kDa). A comparison of 90-11, 27-37, and 90-12, 8-14 (Table I) showed that, when compared on the basis of B9 bioactivity, the former registered higher in the 7IL-6/5IL-6 ELISA than the latter. However, neither the B9 assay nor the ELISA data were correlated with the results of Western blot analyses (Table I). The strongest IL-6 signals in Western blots were observed in the flow-through of baboon 90-11, 3-14 (150-400 kDa) and the flow-through of baboon 90-12, 8-14 (150-300 kDa) (Fig. 3A). The detection of IL-6 species at high concentrations in sample 90-11, 3-14 FT by Western blotting is remarkable because it corresponds to very weak B9 and ELISA signals in Figure 2 and Table I. We have previously verified by direct N-terminal amino acid sequencing that serum-derived proteins such as those illustrated in the Western blot in Figure 3A are indeed IL-6 (13).

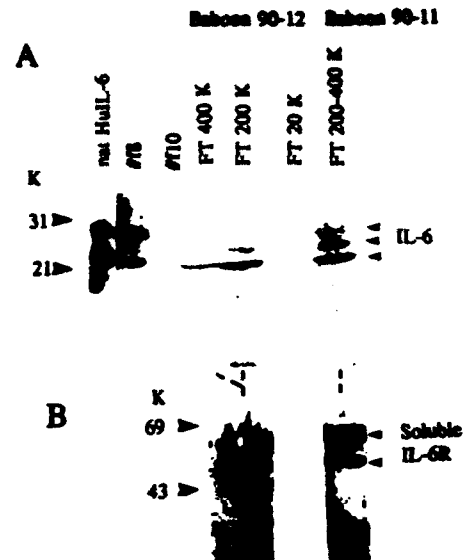


**FIGURE 3.** Western blot analyses of IL-6 and soluble IL-6 receptor present in high molecular mass complexes in baboon plasma. **A**, Aliquots of 0.3 ml of each of the fractions enumerated in Table I were lyophilized, resuspended in solubilizing buffer, subjected to SDS-PAGE and Western blot analyses using a rabbit anti-rHuIL-6 antiserum. For comparison, 15 ng of natural human IL-6 was also included ("nat HuIL-6"). (#8 and #10 correspond to fractions 8 and 10 in Figure 2, baboon 90-12; FT 400 kDa, FT 200 kDa, and FT 20 kDa of baboon 90-12 correspond to the flow-through fractions of the 300 to 400 kDa, 150 to 300 kDa, and 15 to 25 kDa pools of baboon 90-12 in Table I; FT 200 to 400 kDa corresponds to the flow-through of the 200 to 400 kDa pool of baboon 90-11 in Table I. **B**, Pools corresponding to the 200 to 400 kDa gel filtration fractions of baboon 90-11 and 90-12 (see Fig. 2) were passed through an anti-IL-6 receptor mAb (MT-18) immunoaffinity column and an aliquot of adsorbed/eluted material analyzed for soluble IL-6 receptor species by SDS-PAGE under reducing and denaturing conditions and Western blotting using anti-IL-6R mAb MT-18 as the probe.

Furthermore, in a manner consistent with our previous description of human IL-6 complexes (13), the 200- to 400-kDa complexes from both baboons 90-11 and 90-12 contained sIL-6R (Fig. 3B). Thus it is clear that 1) IL-6 exists largely in high molecular mass complexes in both baboons 90-11 and 90-12, and 2) that B9 and ELISA reactivities do not adequately reflect the concentrations of IL-6 present in serum/plasma. The occurrence of baboon IL-6 in complexes with other circulating proteins, including sIL-6R species, drastically alters its B9 activity and ELISA reactivity.

Passive immunization of baboon 90-12 with anti-IL-6 mAb did not appear to significantly alter any of the physiologic and hemodynamic alterations such as hypotension, tachycardia, and increased lacticacidemia produced by LPS as compared to the control baboon 90-11 (data not shown).

**Table II**  
Effect of preinjection of anti-IL-6 mAb on serum IL-6 and fibrinogen levels in mice administered TNF<sup>a</sup>

Experimental Group	Inducer	mAb	IL-6 (B9 U/ml) at 13-14 h	Fibrinogen (mg/dl)
				at 13-14 h (mean ± SD)
1.	Saline		<4	138 ± 43
2.	Saline	GL113	4	229 ± 33
3.	Saline	20F3	13	156 ± 20
4.	TNF		5	350 ± 62
5.	TNF	GL113	3	362 ± 11
6.	TNF	20F3	9,115	131 ± 5 <sup>b</sup>

<sup>a</sup> Anti-MuIL-6 mAb (20F3) or control mAb (GL113) 600 µg/mouse administered i.p. before the inducers; TNF 5 µg/mouse administered i.p.

<sup>b</sup>  $p < 0.02$  comparing groups 5 and 6 using the Student's *t*-test and ANOVA.

### Anti-MuIL-6 mAb in mouse

Mice administered TNF together with a control rat mAb (GL113) showed clear elevations of fibrinogen levels at 13 to 14 h after the cytokine challenge; by 13 to 14 h only trace levels of serum IL-6 were still detectable in these control animals (Table II). In contrast, mice preinjected with the anti-MuIL-6 mAb (20F3) showed elevated sustained B9 bioactivity in the circulation but a reduction in the induction of fibrinogen compared to the mAb controls (Table II). Thus there was a clear dissociation between the levels of circulating IL-6 and the *in vivo* fibrinogen response (Table II).

Could anti-IL-6 mAb block clearance of the induced IL-6 or did Ag/antibody complexes induce more endogenous IL-6? We attempted to obtain evidence that would point to one or the other hypothesis by asking how rapidly did the enhancement of circulating IL-6 occur in the anti-MuIL-6 mAb-treated mouse. Table III shows that marked paradoxical increases in circulating IL-6 bioactivity were observed in anti-MuIL-6 mAb-pretreated mice as early as 2 to 3 h after administration of the inducer (either TNF, IL-1, or LPS). All of the B9 bioactivity described in Tables II and III, even in sera from anti-MuIL-6-treated animals, could be completely neutralized in cell culture by the further addition of anti-MuIL-6 mAb 20F3 (data not shown).

That the marked paradoxical enhancement of IL-6 levels in anti-IL-6 mAb- and IL-6-inducer-treated animals was observed as early as 2 to 3 h after the inducer (Table III) suggested that a simple block in IL-6 clearance from the circulation was not the complete explanation. Could the IL-6 Ag/anti-IL-6 mAb complex *per se* be an efficient inducer of IL-6 *in vivo*? Furthermore, could the circulating IL-6 be in a complex that was not bioavailable *in vivo*, even though it had clear-cut *ex-vivo* B9 activity?

### Exogenous rIL-6/anti-IL-6 mAb complexes in mouse

Table IV summarizes data from a representative experiment in which either murine rIL-6 or rHuIL-6 complexes together with their cognate mAb were administered *i.p.*

**Table III**  
Effect of preinjection of anti-IL-6 mAb on serum IL-6 levels in mice administered TNF or IL-1 or LPS<sup>a</sup>

Experimental Group	Inducer	mAb	IL-6 (B9 U/ml)		
			3 h	6 h	18 h
1.	Saline		<4	13	<2
2.	TNF		1,609	171	2
3.	TNF	GL113	1,316	193	<2
4.	TNF	20F3	7,848	20,638	2,684
5.	IL-1		439	11	<2
6.	IL-1	GL113	94	<2	<2
7.	IL-1	20F3	2,092	402	52
8.	Saline <sup>b</sup>		9		
9.	LPS <sup>b</sup>		6,624		
10.	LPS <sup>b</sup>	GL113	6,812		
11.	LPS <sup>b</sup>	20F3	65,341		

<sup>a</sup> Anti-MuIL-6 mAb (20F3) or control mAb (GL113) mAb (600 µg/mouse) were administered *i.p.* before the inducers. TNF 5 µg or IL-1 20 ng or LPS 5 µg per mouse were administered *i.p.*

<sup>b</sup> The LPS data are at 2 h after administration of the inducer.

**Table IV**  
Serum IL-6 levels in mice injected with mixtures of rMu or rHuIL-6 and anti-MuIL-6 or anti-HuIL-6 mAb<sup>a</sup>

Experimental Group	Ag	mAb	IL-6 (B9 U/ml)		Fibrinogen (mg/dl) at 18-20 h (mean ± SD)
			30 min	120 min	
1.	Saline		<4		242 ± 4
2.	rMuIL-6		207	43	329 ± 8
3.	rMuIL-6	20F3	5,495	13,688	425 ± 14 <sup>b</sup>
4.	rMuIL-6	GL113	718	86	335 ± 23
5.		5IL6-H17	<4	<4	207 ± 24
6.	rHuIL-6	5IL6-H17	8,377	14,644	496 ± 65 <sup>c</sup>
7.	rHuIL-6		979	280	337 ± 81

<sup>a</sup> rIL-6 1.25 µg/mouse; anti-MuIL-6 mAb (20F3) and control mAb (GL113) 100 µg/mouse; anti-HuIL-6 (5IL6-H17) 100 µg/mouse. mAb and rIL-6 were premixed before injection *i.p.*

<sup>b</sup>  $p < 0.05$  comparing group 3 with either group 2 or group 4 using Student's *t*-test and ANOVA.

<sup>c</sup>  $p < 0.05$  comparing group 6 with either group 5 or group 7 using Student's *t*-test and ANOVA.

Markedly elevated levels of IL-6 were seen in the murine circulation as early as 30 min after instillation of the Ag/mAb complexes. There were commensurate increases in circulating fibrinogen levels in the murine rIL-6/anti-murine IL-6 mAb and the rHuIL-6/anti-HuIL-6 mAb-treated animals. Clearly, this rapid appearance of IL-6 in the murine circulation was not likely to be due to new synthesis of IL-6 nor due to a block in IL-6 "clearance." Table IV shows that the fibrinogen response elicited in the mouse by a combination of IL-6 and its "neutralizing" mAb was more than that observed using rIL-6 alone.

The possibility that the rapid release of IL-6 into the murine circulation in experiments such as in Table IV was from a presynthesized murine store such as an endothelial cell reservoir, was examined in experiments in which the IL-6 present in the murine circulation was serotyped. If the circulating IL-6 were derived from a murine store then IL-6 in mice administered rHuIL-6/5IL6 mAb should be of the murine serotype. Table V summarizes the result of a representative IL-6 serotyping experiment. The IL-6 seen in

Table V  
Serotyping of circulating IL-6 in mice administered rIL-6/anti-IL-6 mAb mixtures (in Table IV)

Sample	Residual IL-6 Titer (B9 U/ml)			
	Preimmune serum	anti-MuIL-6 serum	control mAb (IgG1)	anti-HuIL-6 mAb (5IL6-H17)
rMuIL-6/anti-MuIL-6 (20F3), 30 min	9,404	<10 <sup>a</sup>	11,233	11,009
rHuIL-6/anti-HuIL-6 (5IL6), 30 min	11,862	11,662	12,987	33
rMuIL-6/anti-MuIL-6 (20F3), 120 min	17,861	<10 <sup>a</sup>	20,231	20,390
rHuIL-6/anti-HuIL-6 (5IL6), 120 min	29,469	29,356	24,898	65 <sup>b</sup>
Serotyping controls				
rMuIL-6	5,275	<10 <sup>a</sup>	5,850	5,304
rHuIL-6	1,447	1,569	1,515	<10

<sup>a</sup> Titer reflects biologic activity of minimally diluted mixtures of sample and antiserum. Partial activity is recovered on dilution of the antibody/sample mixture by another 25- to 100-fold (see comment in text).

<sup>b</sup> Shallow slope in the bioassay.

the circulation in the mice in Table IV was presynthesized in the laboratory. The circulating IL-6 was of the same serotype that had been used in the injection mixture. Under these experimental conditions the presence of anti-IL-6 mAb in the injected complexes appeared to have at least three effects: 1) rapid entry of rIL-6 from the peritoneum into the peripheral circulation, 2) long-term maintenance of IL-6 levels in the peripheral circulation, and 3) enhanced elicitation of a fibrinogen response. So-called "neutralizing" anti-IL-6 mAb served to chaperone rIL-6 into (and around) the peripheral circulation, and surprisingly up-regulated IL-6 biologic activity in vivo. That the murine rIL-6 and the anti-IL-6 mAb in the sera of animals injected i.p. with IL-6/mAb complexes is in a state of dynamic equilibrium is suggested by the observation that although the addition of rabbit anti-murine rIL-6 antiserum blocked B9 bioactivity in cell culture assays (as in Table V), further dilution of the Ab/test sample mixtures resulted in a partial reappearance of B9 proliferation activity (data not shown).

What was the stoichiometry needed to observe the chaperone effect of anti-IL-6 mAb on rIL-6 compared to that required for a reduction in the in vivo fibrinogen response? Mixtures containing a constant amount of rHuIL-6 and different amounts of anti-HuIL-6 mAb were administered i.p. into mice and the circulating B9 bioactivity was determined 2 h later, and the fibrinogen response measured 18 h later (Fig. 4). It is clear from the data in Figure 4 that a molar ratio of Ag to mAb of 1:1 was sufficient to observe the chaperone effect of anti-IL-6 mAb. A ratio of 1:1 was near-maximal in eliciting enhanced in vivo fibrinogen response and enhancing circulating IL-6 levels. A ratio of 1:125 blocked the enhanced fibrinogen response even though the circulating B9 bioactivity was elevated. Thus, under these conditions not all the ex vivo measurable circulating IL-6 was available in vivo to elicit an hepatocyte response. The inhibition of the fibrinogen response using anti-IL-6 mAb at ratios of 1:25 to 1:125 is all the more striking because it is to be compared to the enhancement of fibrinogen levels produced by the isotype-matched control mAb. That administration of 120 or 600  $\mu$ g of a "control" mAb into mice

enhanced fibrinogen levels suggests that the control mAb at these doses can itself induce endogenous murine IL-6. Indeed, not only was circulating IL-6 detected in mice even 18 h after administration of 600  $\mu$ g of control mAb (Fig. 4B legend), but also that the serotype of this IL-6 was consistent with its being endogenous murine IL-6 (not shown).

#### Biochemical characterization of IL-6 in murine circulation

B9 bioassay data for IL-6 levels in the murine circulation corresponded to IL-6 amounts that could be verified by Western blotting. Thus, in Western blots using the appropriate anti-rHuIL-6 or anti-murine rIL-6 rabbit antisera, the expected amounts of rHuIL-6 Ag were observed in sera of animals administered rHuIL-6/anti-HuIL-6 mAb complexes in Figure 4, and the expected amounts of murine IL-6 Ag were observed in sera of mice injected LPS and 20F3 in Table III (data not shown). Figure 5 summarizes the results of several G-200 gel-filtration analyses of IL-6 in the murine circulation in representative experimental groups. Figure 5A shows that B9 active IL-6 in a mouse administered LPS was largely of low molecular mass (20 kDa), but that IL-6 from a mouse pretreated with anti-murine IL-6 mAb (20F3) and then administered LPS was largely of high molecular mass (200 kDa). The data in Figure 5B reconfirm that IL-6 in anti-murine IL-6 and LPS-treated mice was high molecular mass (200 kDa) and show that circulating IL-6 in a mouse administered a complex of both murine rIL-6 and anti-MuIL-6 mAb was also 200 kDa. Figure 5C reports that in a mAb-free mouse, B9-bioactive rHuIL-6 behaved largely as a low molecular mass species (15–20 kDa). In contrast, the B9-bioactive and ELISA-reactive rHuIL-6 administered in association with anti-HuIL-6 mAb (5IL6-H17) was largely high molecular mass (200 kDa) (Fig. 5C). Taken together, Figure 5 shows that circulating IL-6 in the anti-IL-6 mAb-treated mouse, as in the baboon (Fig. 2), behaved as a high molecular mass complex of size 200 kDa.

### Hepatocyte stimulating activity of murine circulation-derived IL-6

What is the ability of IL-6 in the murine circulation to stimulate fibrinogen synthesis in cell cultures of the rat hepatoma line Reuber H35? The ability of sera from animals receiving injections with IL-6/anti-IL-6 mAb complexes (Table IV, groups 3 and 6) to stimulate fibrinogen synthesis in cultures of H35 hepatoma cells is illustrated in Figure 6A. All four sera pools from animals in Table IV, groups 3 and 6 (both 30- and 120-min groups) were able to elicit a strong enhancement of fibrinogen synthesis and secretion in H35 hepatoma cells. The further addition of anti-murine rIL-6 rabbit Ab did not affect the fibrinogen response (Fig. 6A). This is remarkable because Table V shows that the addition of the same rabbit anti-murine rIL-6

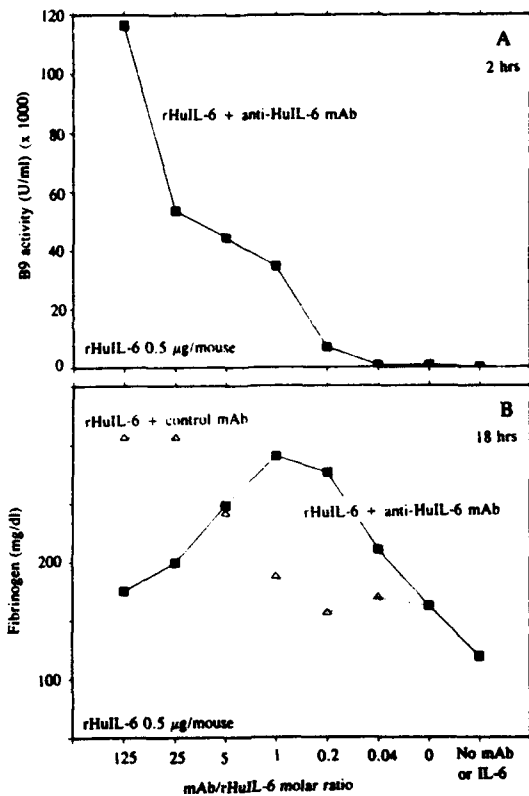


**FIGURE 4.** Consequences of administering rHuIL-6/anti-HuIL-6 mAb complexes i.p. into mice. Mice received varying amounts (different molar ratios) of anti-HuIL-6 mAb (5IL6-H17) or a control mAb mixed with a constant amount (0.5  $\mu$ g) of rHuIL-6. **A**, Circulating IL-6 titers as measured in the B9 bioassay at 2 h after administering the IL-6/anti-IL-6 complexes (■). **B**, Fibrinogen levels in serum at 18 h after administering either the IL-6/anti-IL-6 complexes (■) or the IL-6/control mAb (○) mixtures. At 18 h the IL-6 titers (B9 bioassay in U/ml) in sera of mice given IL-6/anti-IL-6 complexes (molar ratio in parentheses) were 7634 (125), 9713 (25), 2734 (5), 175 (1), 18 (0.2), and 8 (0.04); the corresponding titers in animals administered rHuIL-6 and control mAb were 9 (125), <4 (25), <4 (5), <4 (1), <4 (0.2), <4 (0.04), <4 (0), and <4 (no mAb or IL-6).

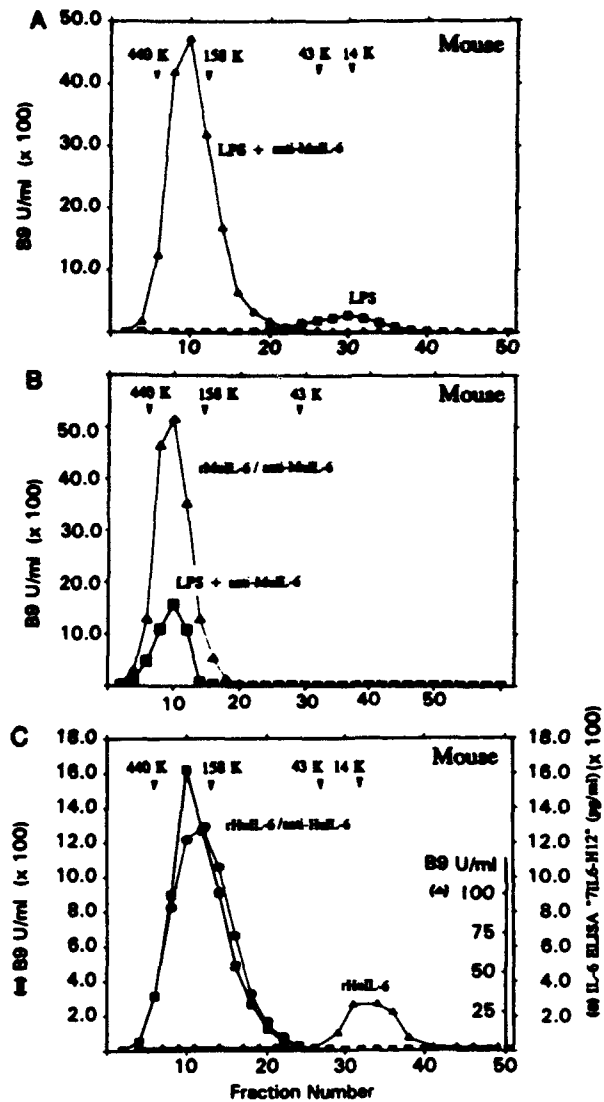


**FIGURE 5.** Sephadex G-200 gel filtration analyses of IL-6 present in murine serum. Aliquots (1 ml) of murine sera corresponding to different experimental groups were subjected to G-200 gel filtration chromatography. The eluted fractions were assayed in the B9 bioassay, an appropriate ELISA, or in the hepatocyte assay (as in Fig. 6). **A**, Serum IL-6 B9 bioactivity in mice 2 h after administration of LPS without (■) or with preinjection of anti-MuIL-6 mAb 20F3 (○). **B**, Serum IL-6 B9 bioactivity in mice preinjected with anti-MuIL-6 mAb (20F3) (○) and then bled 2 h after administration of LPS (■), or 2 h after coinjection of murine rIL-6 and anti-murine IL-6 mAb (20F3) (□). **C**, Serum IL-6 B9 bioactivity in mice 1 h after administration of rHuIL-6 (○; right y-axis) or 2 h after administration of rHuIL-6/anti-HuIL-6 mAb complexes (■; left y-axis). The latter fractions were also reassayed using the 7IL6/5IL6 ELISA (●).

Ab to samples from Table IV, group 3 (30- and 120-min groups) inhibited the IL-6 bioactivity in the B9 assay. Taken together, the data point to a dissociation between the ability of anti-murine rIL-6 Ab to inhibit IL-6-mediated hepatocyte stimulation compared to B9 proliferation.

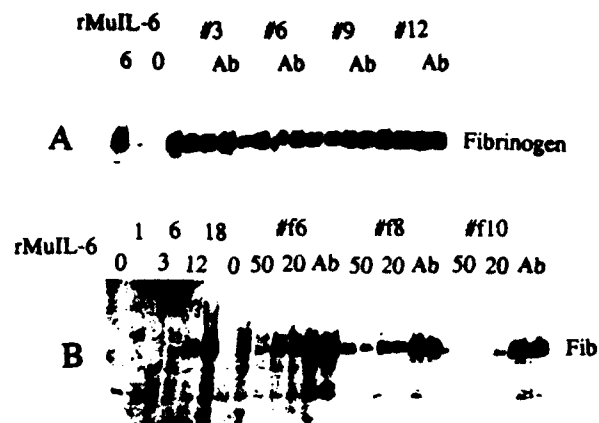


**FIGURE 6.** Stimulation of fibrinogen synthesis and secretion by H35 Reuber hepatoma cells in response to mouse-serum-derived IL-6. In the experiments in *A* and *B*, recombinant baculovirus-vector-derived murine rIL-6 was used as the assay standard; concentrations are expressed in ng/ml. *A*, Duplicate lanes show the stimulation of fibrinogen synthesis using a 1/20 dilution of sera from groups 3 (3, 30 min and 9, 120 min) and 6 (6, 30 min and 12, 120 min) of Table IV. In 3 and 9 a complex of murine rIL-6/anti-murine IL-6 mAb was administered, and in 6 and 12 a complex of rHuIL-6/anti-HuIL-6 mAb was administered. Duplicate lanes marked Ab include 1/100 dilution of a rabbit-anti-murine rIL-6 serum (comparable to the B9 neutralization data in Table V). *B*, Duplicate lanes marked (50, 20, or Ab) show stimulation of fibrinogen synthesis in H35 cells in response to a 1/50 dilution, a 1/20 dilution, or a 1/50 dilution plus Ab (1/100 dilution of rabbit anti-murine rIL-6) of G-200 elution fractions 6, 8, and 10 (f6, f8, or f10) derived from the murine rIL-6/anti-murine IL-6 coinjection (2 h) group in Figure 5B.

Do high molecular mass, B9-bioactive murine IL-6 complexes have hepatocyte stimulating activity? Aliquots of individual fractions across the 200- to 300-kDa peak were assayed for their ability to stimulate fibrinogen synthesis in H35 Reuber cells (Fig. 6B). Figure 6B illustrates that each of the high molecular mass fractions assayed (f6, f8, f10) enhanced fibrinogen synthesis in H35 cells. Paradoxically, the addition of "neutralizing" (in the B9 bioassay) rabbit anti-murine rIL-6 Ab markedly enhanced the fibrinogen stimulation observed, perhaps because of its ability to free IL-6 from its complexes. In other experiments we have observed that control Ag/Ab complexes do not enhance fibrinogen synthesis in Reuber H35 cells (data not shown). The observations summarized in Figure 6 prompt the question: does anti-murine IL-6 mAb 20F3 neutralize the activity of murine rIL-6 in the H35 Reuber hepatoma assay? When murine rIL-6 was mixed with mAb 20F3 at different molar ratios in the range 1:125 to 1:0.04 and the mixtures then assayed in both the H35 hepatoma assay and in the B9 proliferation assay, the mAb 20F3 blocked the activity of murine rIL-6 in the B9 assay at a molar ratio of 1:1 or higher, but left unaffected or even enhanced the ability of murine rIL-6 to stimulate fibrinogen synthesis in the hepatocyte assay (data not shown). We have also observed that

rabbit anti-murine IL-6 Ab enhanced the ability of murine rIL-6 to stimulate fibrinogen synthesis in H35 cells although inhibiting any B9 cell growth activity (data not shown). Thus, the inhibition of the fibrinogen response by preinjected anti-murine IL-6 mAb (20F3) *in vivo* (Table II) may not reflect an intrinsic "neutralization" of the hepatocyte activity of endogenous murine IL-6, but a sequestration of murine IL-6 in the intravascular compartment. Taken together, the data presented in this article suggest the existence of a novel level of regulation of IL-6 action *in vivo*—that of regulating the access of IL-6 to its target hepatic tissue.

## Discussion

In this study we address several essential questions concerning the paradoxical *in vivo* effects of anti-IL-6 neutralizing antibodies. First, we examine the biochemical characteristics, size, and form of IL-6 in circulation of animals (baboon and mice) receiving the antibody. Second, we evaluate the effects of administering "neutralizing" antibodies to IL-6 *in vivo* as indicated by the uniquely specific pathophysiologic function of IL-6 of inducing fibrinogen in hepatocytes (11, 12), with simultaneous determination of IL-6 levels, size, and form in circulation. Third, given the dissociation between the apparent abrogation with preinjected antibody of *in vivo* IL-6 effects and the increased and sustained presence of the cytokine in circulation in a complexed form, we evaluate whether preformed rHuIL-6/mAb or murine rIL-6/mAb complexes show similar dichotomy in their effects. Fourth, we determine whether the presence of enhanced levels of circulating IL-6 occurs through induction and/or release of endogenous IL-6.

The results in this study extend our previous findings showing that IL-6 exists in the peripheral circulation in the form of complexes with other proteins (13). The new data in the baboon are in line with our earlier conclusion that natural human IL-6 exists in plasma or serum in high molecular mass complexes that contain additional proteins (fragments of CRP, C3, C4 and soluble IL-6 receptor gp80). In the two experimental species used in our study (baboon and mouse), "neutralizing" anti-IL-6 mAb had the unexpected property of chaperoning IL-6 (perhaps together with other associated proteins) into and around the peripheral circulation leading to a paradoxical sustained elevation of circulating IL-6. In animals passively immunized with anti-IL-6 mAb, there appeared to exist a dynamic equilibrium involving IL-6 Ag, IL-6 bioactivity, mAb, and IL-6/mAb complexes. In this situation, depending on the molar ratio of Ag to antibody, anti-IL-6 mAb could either enhance or inhibit the ability of IL-6 present in the intravascular compartment to elicit hepatocyte effects *in vivo* (e.g., stimulation of fibrinogen levels), even though there was a uniform elevation of intravascular IL-6 bioactivity. Instillation of a mixture of rIL-6 and anti-IL-6 mAb *i.p.* into mice

showed that a 1:1 ratio between Ag and antibody was essentially sufficient for the chaperoning effect. The net effect of mAb was to enhance the speed and the magnitude with which rIL-6 instilled i.p. entered the peripheral circulation, and the duration that it remained in the peripheral circulation. In essence, surprisingly, anti-IL-6 mAb enhanced the *in vivo* biologic potency of exogenously administered rIL-6 at least with respect to the fibrinogen response.

Convincing passive immunization experiments using anti-IL-6 mAb in animal models have been difficult. Vink et al. (14) reported that an anti-murine IL-6 mAb and/or an anti-murine IL-6R mAb administered *in vivo* were able to inhibit the growth of an IL-6-dependent plasmacytoma tumor (14). Strassmann et al. (16) reported that the anti-murine IL-6 mAb 20F3 reduced tumor-induced cachexia in rodent models; these authors reported that circulating IL-6 levels were only partially reduced in this "chronic" induction situation. Neta et al. (20) have confirmed the ability of 20F3 to inhibit the stimulation of fibrinogen and to block the hypoglycemic response and the endocrine response (elevations of serum cortisone and ACTH) in mice administered LPS, TNF, or IL-1 (20, 31). In contrast, Mihara et al. (32) reported that an anti-IL-6 mAb enhanced the stimulation of circulating Ig levels in mice in response to rIL-6 administration.

Our previous results showed that anti-HuIL-6 mAb 5IL6-H17 led to enhanced circulating levels of IL-6 in animals administered IL-6 inducers (17). Paradoxical elevation of biologically assayed IL-6 levels in anti-IL-6 mAb-treated animals concomitant with a reduction in LPS-induced pathophysiologic effects has also been reported (19). The detection of B9-bioassay-active complexes of anti-IL-6 mAb and IL-6 in sera of anti-IL-6 mAb-treated myeloma patients has also been described (18).

In our study mAb against murine IL-6 given to mice before IL-6 inducer, reduced the levels of fibrinogen in circulation, whereas the same antibody given complexed with murine rIL-6 resulted in a greater response. Stimulation of the fibrinogen response *in vivo* by IL-6 in the latter animals was crucially dependent on the molar ratio between Ag and antibody. Under appropriate experimental conditions (Ag to mAb ratio approximately 1:125) there was a dissociation between the ability of *in vivo*-derived IL-6 to stimulate plasma protein synthesis in hepatocytes (decreased) and to stimulate B9 cell proliferation (increased). That IL-6 existed in the mAb-treated animals *in vivo* as part of a large complex of approximate molecular mass 200-kDa provides an example of how "associated" proteins can modulate the pharmacology and function of this cytokine.

That anti-IL-6 mAb enhanced the rapid entry of rIL-6 from the peritoneal cavity into the peripheral circulation in less than 30 min points to the existence of an unusual mechanism for handling cytokine/mAb complexes. The present data indicate that a molar ratio of 1:1 between Ag and antibody suffices for IL-6 to be chaperoned efficiently

into the circulation. Is it possible that there exist proteins other than mAb that serve this chaperone function *in vivo*? The demonstration that the bulk of IL-6 in mAb-free baboon plasma as assayed by Western blotting exists in a complex of mass 400 kDa suggests that the answer to this question is yes. Conceptually, it would indeed be an advantage if specific proteins were able to physiologically chaperone a "systemic" cytokine such as IL-6 from its sites of local production (local infection or tissue injury) into the peripheral circulation. That IL-6 ordinarily exists as a high molecular mass complex in human and baboon plasma (even in the absence of mAb) points to the existence of other cytokine chaperones. The ability of anti-IL-6 Ab to "unmask" and enhance IL-6 bioactivity in H35 hepatoma cells, but not the B9 cell, bioassay from such complexes (Fig. 6) is an unexpected result that is suggestive of the presence of inhibitory IL-6 chaperones *in vivo*.

Although our report deals exclusively with IL-6 and its interactions with other proteins in the peripheral circulation, the data lead us to consider the more general question of cytokine chaperones. Finkelman et al.<sup>4</sup> have recently reported that anti-IL-4 mAb can also enhance the biologic effects of IL-4 *in vivo*. Thus, mAb-mediated chaperoning of cytokines may be a general phenomenon. Do chaperone proteins other than mAb exist for other cytokines? Clearly the presence of soluble circulating receptors for various cytokines suggests that the answer is yes. The possibility that other nonreceptor proteins are involved in the transport of cytokines *in vivo* opens up a new area of research. The related question of bioavailability of cytokines *in vivo* as distinct from its biologic activity as measured *ex vivo* in different assays is an important one. This question takes on added significance as various cytokines, in particular IL-6, move into the clinic as therapeutic agents (33).

## Acknowledgments

The authors thank Dr. Eva Fischer for assistance with the baboon experiments and Natalie Davis for help with the murine experiments.

## References

1. Fong, Y., L. L. Moldawer, G. T. Shires, and S. F. Lowry. 1990. The biologic characteristics of cytokines and their implication in surgical injury. *Surg. Gynecol. Obstet.* 170:363.
2. Tracey, K. J., Y. Fong, D. G. Hesse, K. R. Manogue, A. T. Lee, G. C. Kuo, S. F. Lowry, and A. Cerami. 1987. Anti-cachectin/TNF monoclonal antibodies prevent septic shock during lethal bacteremia. *Nature* 330:662.
3. Fong, Y., K. J. Tracey, L. L. Moldawer, D. G. Hesse, K. B. Manogue, J. S. Kenney, A. T. Lee, G. C. Kuo, A. C. Allison, S. F. Lowry, and A. Cerami. 1989. Antibodies to cachectin/TNF reduce IL-1 $\beta$  and IL-6 appearance during lethal bacteremia. *J. Exp. Med.* 170:1627.

<sup>4</sup> Finkelman, F. D., K. B. Madden, S. C. Morris, J. M. Holmes, N. Boiani, I. M. Katona and C. R. Maliszewski. Anti-cytokine antibodies as carrier proteins: prolongation of *in vivo* effects of exogenous cytokines by injection of cytokine-anticytokine antibody complexes. *J. Immunol.* *In press.*

4. Havell, E. A., and P. B. Sehgal. 1991. TNF-independent IL-6 production during murine listeriosis. *J. Immunol.* 146:756.
5. Havell, E. A., L. L. Moldawer, D. Helfgott, P. L. Kilian, and P. B. Sehgal. 1992. Type I IL-1 receptor blockade exacerbates murine listeriosis. *J. Immunol.* 148:1486.
6. Neta, R., J. J. Oppenheim, R. D. Schreiber, R. Chizzonite, G. D. Ledney, and T. J. MacVittie. 1991. Role of cytokines (IL-1, TNF and TGF- $\beta$ ) in natural and lipopolysaccharide-enhanced radioresistance. *J. Exp. Med.* 173:1177.
7. Gershenwald, J. E., Y. Fong, T. J. Fahey III, S. E. Calvano, R. Chizzonite, P. L. Kilian, S. F. Lowry, and L. L. Moldawer. 1990. IL-1 receptor blockade attenuates the host inflammatory response. *Proc. Natl. Acad. Sci. USA* 87:4966.
8. Gresser, I., M. G. Tovey, M. -T. Bandu, C. Maury, and D. Brouty-Boye. 1976. Role of interferon in the pathogenesis of virus diseases in mice as demonstrated by the use of anti-interferon serum. *J. Exp. Med.* 144:1305.
9. Havell, E. A. 1986. Augmented induction of interferons during *Listeria monocytogenes* infection. *J. Infect. Dis.* 253:960.
10. Riviere, Y., I. Gresser, J. -C. Guillon, and M. G. Tovey. 1977. Inhibition of anti-interferon serum of lymphocytic choriomeningitis virus disease in suckling mice. *Proc. Natl. Acad. Sci. USA* 74:2135.
11. Sehgal, P. B., G. Grieninger, and G. Tosato. 1989. Regulation of the acute phase and immune responses: interleukin-6. *Ann. N.Y. Acad. Sci.* 557:1.
12. Heinrich, P. C., J. V. Castell, and T. Andus. 1990. IL-6 and the acute phase response. *Biochem. J.* 265:621.
13. May, L. T., H. Viguet, J. S. Kenney, N. Ida, A. C. Allison, and P. B. Sehgal. 1992. High levels of "complexed" interleukin-6 in human blood. *J. Biol. Chem.* 267:19698.
14. Vink, A., P. Coulie, G. Warnier, J. -C. Renaud, M. Stevens, D. Donckers, and J. Van Snick. 1990. Mouse plasmacytoma growth in vivo: enhancement by IL-6 and inhibition by antibodies directed against IL-6 or its receptor. *J. Exp. Med.* 172:997.
15. Aarden, L. A., and C. van Kooten. 1992. The action of IL-6 on lymphoid populations. *CIBA Found. Symp.* 167:68.
16. G. Strassmann, M. Fong, J. S. Kenney, and C. O. Jacob. 1992. Evidence for the involvement of IL-6 in experimental cancer cachexia. *J. Clin. Invest.* 89:1681.
17. Sehgal, P. B. 1992. Discussion. *CIBA Found. Symp.* 167:186.
18. Lu, Z. Y., J. Brochier, J. Wijdenes, H. Brailly, R. Bataille, and B. Klein. 1992. High amounts of circulating IL-6 in the form of monomeric immune complexes during anti-IL-6 therapy. Towards a new methodology for measuring overall cytokine production in human in vivo. *Eur. J. Immunol.* 22:2819.
19. Heremans, H., C. Dillen, W. Put, J. Van Damme, and A. Billiau. 1992. Protective effect of anti-IL-6 antibody against endotoxin, associated with paradoxically increased IL-6 levels. *Eur. J. Immunol.* 22:2395.
20. Neta, R., R. Perlstein, S. N. Vogel, G. D. Ledney, and J. Abrams. 1992. Role of IL-6 in protection from lethal irradiation and in endocrine responses to IL-1 and TNF. *J. Exp. Med.* 175:689.
21. Fischer, E., M. A. Marano, K. J. Van Zee, C. S. Rock, A. S. Hawes, W. A. Thompson, L. DeForge, J. S. Kenney, D. G. Remick, D. C. Bloodow, R. C. Thompson, S. F. Lowry, and L. L. Moldawer. 1992. IL-1 receptor blockade improves survival and hemodynamic performance in *E. coli* septic shock, but fails to alter host responses to sublethal endotoxemia. *J. Clin. Invest.* 89:1551.
22. Starnes, H. F., M. K. Pearce, A. Tewari, J. H. Yim, J. C. Zou, and J. Abrams. 1990. Anti-IL-6 monoclonal antibodies protect against lethal *Escherichia coli* infection and lethal TNF challenge in mice. *J. Immunol.* 145:4185.
23. Aarden, L. A., P. M. Lansdorp, and E. R. de Groot. 1985. A growth factor for B-cell hybridomas produced by human monocytes. *Lymphokines* 10:175.
24. Santhanam, U., C. Avila, R. Romero, H. Viguet, N. Ida, S. Sakurai, and P. B. Sehgal. 1991. Cytokines in normal and abnormal parturition: elevated amniotic fluid IL-6 levels in women with premature rupture of membranes associated with intrauterine infection. *Cytokine* 3:155.
25. Helfgott, D. C., S. B. Tatter, U. Santhanam, R. H. Clarick, N. Bhardwaj, L. T. May, and P. B. Sehgal. 1989. Multiple forms of IFN- $\beta_2$ /IL-6 in serum and body fluids during acute bacterial infections. *J. Immunol.* 142:948.
26. Kenney, J. S., M. P. Masada, E. M. Eugui, B. M. Delustro, M. A. Mulkins, and A. C. Allison. 1987. Monoclonal antibodies to human recombinant IL-1 $\beta$ : quantitation of IL-1 $\beta$  and inhibition of biological activity. *J. Immunol.* 138:4236.
27. Laemmli, U. K. 1970. Cleavage of structural proteins during the assembly of the head of the bacteriophage T4. *Nature* 227:680.
28. Towbin H., T. Staehelin, and J. Gordon. 1979. Electrophoretic transfer of proteins from polyacrylamide gels to nitrocellulose sheets: procedure and some applications. *Proc. Natl. Acad. Sci. USA* 76:4350.
29. May, L. T., J. Ghayeb, U. Santhanam, S. B. Tatter, Z. Sthoeger, D. C. Helfgott, N. Chiorazzi, G. Grieninger, and P. B. Sehgal. 1988. Synthesis and secretion of multiple forms of " $\beta_2$ -interferon/B-cell differentiation factor BSF-2/hepatocyte stimulating factor" by human fibroblasts and monocytes. *J. Biol. Chem.* 263:7760.
30. Taga, T., M. Hibi, Y. Hirata, K. Yamasaki, K. Yasukawa, T. Masuda, T. Hirano, and T. Kishimoto. 1989. Interleukin-6 triggers the association of its receptor with a possible signal transducer, gp130. *Cell* 58:573.
31. Perlstein, R. S., M. H. Whitnall, J. S. Abrams, E. H. Mougey, and R. Neta. 1993. Synergistic roles of IL-6, IL-1 and TNF in the adrenocorticotropin response to bacterial lipopolysaccharide in vivo. *Endocrinology* 132:946.
32. Mihara, M., Y. Koishihara, H. Fukui, K. Yasukawa, and Y. Ohsugi. 1991. Murine anti-human IL-6 monoclonal antibody prolongs the half-life in circulating blood and thus prolongs the bioactivity of human IL-6 in mice. *Immunology* 74:55.
33. Revel, M. 1992. IL-6: Physiopathology and clinical potentials. *Serono Symp. Publ.* 88:1.

## Adverse Effects of Pefloxacin in Irradiated C3H/HeN Mice: Correction with Glucan Therapy

M. L. PATCHEN,\* I. BROOK, T. B. ELLIOTT, AND W. E. JACKSON

*Departments of Experimental Hematology and Computers and Electronics, Armed Forces Radiobiology Research Institute, Bethesda, Maryland 20889-5603*

Received 14 May 1993/Returned for modification 10 June 1993/Accepted 13 July 1993

**Opportunistic bacterial infections are the predominant cause of death following myelosuppressive radiation exposure. When used alone, a variety of immunomodulators and antibiotics have been reported to reduce radiation-induced death. In these studies, the combined therapeutic effects of the immunomodulator glucan and the quinolone antibiotic pefloxacin were evaluated for survival-enhancing effects in myelosuppressed C3H/HeN mice. Mice were exposed to 7.9 Gy of whole-body <sup>60</sup>Co radiation and treated with saline, glucan (250 mg/kg of body weight intravenously, 1 h after irradiation), pefloxacin (64 mg/kg/day orally, days 3 to 24 after irradiation), or glucan plus pefloxacin. Survival 30 days after irradiation in mice receiving these respective treatments was 25, 48, 7, and 85%. Evaluation of granulocyte-macrophage progenitor cell (GM-CFC) recovery in mice receiving these treatments revealed that, compared with recovery in saline-treated mice, glucan stimulated GM-CFC recovery, pefloxacin suppressed GM-CFC recovery, and glucan administered in combination with pefloxacin could override pefloxacin's hemopoietic suppressive effect.**

Exposure to whole-body radiation induces mortality that is associated with bacteremia caused primarily by endogenous intestinally derived bacteria (1). Previous studies have demonstrated the usefulness of the quinolone pefloxacin in reducing mortality in irradiated B6D2F1 mice (2). The efficacy of pefloxacin was attributed to its activity against facultative intestinal bacterial flora. Pefloxacin may have exerted its antibacterial activity either directly against organisms within the intestinal lumen or systemically against translocated bacteria.

In contrast to previous work with B6D2F1 mice, preliminary studies using pefloxacin therapy in irradiated C3H/HeN mice indicated that pefloxacin therapy actually enhanced mortality after irradiation in these animals. It has been observed that endogenous gastrointestinal bacterial floras differ in these two strains of mice, with more gram-negative enteric aerobic as well as facultative and strict anaerobic organisms present in C3H/HeN mice than in B6D2F1 mice (5a), making the bacterial flora of C3H/HeN mice quantitatively and qualitatively more similar to that of humans. However, mortality following irradiation in both mouse strains results from bacteremia related to their respective intestinally derived bacterial flora. Because pefloxacin is a broad-spectrum antibiotic (14), differences in the endogenous floras of these two mouse strains did not appear to be a reasonable explanation for the survival differences observed in these irradiated mice following pefloxacin treatment. In addition to differences in endogenous flora, C3H/HeN and B6D2F1 mice differ in bone marrow and splenic hemopoietic stem and progenitor cell numbers, with fewer of these cells present in C3H/HeN mice. For example, we have observed that B6D2F1 femoral bone marrow contains approximately 6,500 multipotent spleen CFU and 11,500 granulocyte-macrophage colony-forming cells (GM-CFC) while C3H/HeN femoral bone marrow contains only about 2,000 multipotent spleen CFU and 3,500 GM-CFC (21, 28). Because quinolone antibiotics, including pefloxacin, have been

reported to suppress mammalian cell proliferation (7, 8, 10, 13), we hypothesized that the increased mortality observed following pefloxacin treatment in C3H/HeN mice whose hemopoietic system has already been critically depleted by irradiation may be due to suppressed proliferation of the few surviving hemopoietic stem and progenitor cells.

We have previously demonstrated that glucan, a beta-1,3-polysaccharide immunomodulator, is capable of enhancing hemopoietic regeneration and increasing survival when administered to C3H/HeN mice following irradiation (20, 25, 27). Specifically, glucan therapy has been demonstrated to accelerate repopulation of multipotent hemopoietic stem cells, as well as hemopoietically committed granulocyte-macrophage, pure macrophage, and erythroid progenitor cells. The survival-enhancing and hemopoietic activities of glucan have been correlated with its ability to activate macrophages, resulting in the production of macrophage-derived hemopoietic growth factors as well as enhanced macrophage-mediated defense against opportunistic infections (19, 22, 24). Hence, if pefloxacin were to inhibit hemopoietic regeneration in already critically myelosuppressed mice, glucan therapy may be able to override these suppressive hemopoietic effects while permitting the beneficial antimicrobial effects of pefloxacin to be maintained.

The studies described here were designed to (i) document the deleterious effects of pefloxacin in irradiated C3H/HeN mice, (ii) investigate whether pefloxacin inhibits hemopoietic recovery in C3H/HeN mice following radiation-induced myelosuppression, and (iii) evaluate whether glucan therapy could be used to override the deleterious effects of pefloxacin in irradiated C3H/HeN mice.

### MATERIALS AND METHODS

**Mice.** C3H/HeN female mice (about 25 g) were purchased from Charles River Laboratories (Raleigh, N.C.). Mice were maintained in Micro-Isolator cages (Lab Products, Maywood, N.J.) on hardwood-chip contact bedding and were provided commercial rodent chow and acidified water (pH 2.5) ad libitum. Three days prior to experimentation and

\* Corresponding author.

throughout the experiments, tap water containing 0.03 mg of ascorbic acid per ml was substituted for acidified water. Animal rooms were equipped with full-spectrum light from 0600 to 1800 h and were maintained at  $21 \pm 1^\circ\text{C}$  with  $50\% \pm 10\%$  relative humidity, with at least 10 air changes of 100% conditioned fresh air per h. Upon arrival, all mice were tested for *Pseudomonas* infection and quarantined until test results were obtained. Only healthy mice were released for experimentation. The Institute Animal Care and Use Committee approved all experiments prior to performance. Animals were maintained in a facility accredited by the American Association for the Accreditation of Laboratory Animal Care, and research was conducted according to the principles enunciated in reference 13a.

**Irradiation.** The  $^{60}\text{Co}$  source at the Armed Forces Radiobiology Research Institute was used to administer bilateral total-body gamma radiation. Mice were placed in ventilated Plexiglas containers and irradiated at a dose rate of 0.4 Gy/min. Dosimetry was determined by ionization chambers (31), with standards traceable to the National Institute of Standards and Technology. The tissue-to-air ratio was determined to be 0.96, and the dose variation within the exposure field was <3%.

**Pefloxacin therapy.** Pefloxacin methanesulfonatedihydrate powder (henceforth referred to as pefloxacin) was obtained from Rhone-Poulenc Sante (Antony, France). Pefloxacin therapy was initiated 3 days after irradiation. In dose-response experiments, pefloxacin was prepared in tap water and administered to mice in 0.5-ml volumes at doses of 32, 64, or 320 mg/kg of body weight per day by oral gavage, using a blunt-end 20-gauge feeding needle attached to a 3-ml syringe. In all other experiments, pefloxacin was prepared in tap water at the concentration of 0.6 mg/ml and substituted for tap water in the mouse cage water bottles. As recommended by the manufacturer, 0.03 mg of ascorbic acid per ml was added to the tap water to stabilize pefloxacin activity. Preliminary studies using high-performance liquid chromatography (18) to measure serum pefloxacin levels verified pefloxacin absorption following both oral gavage and water bottle administration. One hour following administration of 64 mg of pefloxacin per kg by oral gavage, the mean serum pefloxacin concentration was  $2.6 \pm 0.4 \mu\text{g/ml}$ ; similarly, mice maintained on pefloxacin-containing tap water for 5 days exhibited a mean serum pefloxacin concentration of  $1.8 \pm 0.5 \mu\text{g/ml}$ . The pefloxacin concentration to be used for water bottle administration was based on preliminary studies in which it was determined that the daily consumption of tap water in mice exposed to 7.9 Gy of  $^{60}\text{Co}$  was approximately 2.6 ml. Hence, pefloxacin at a concentration of 0.6 mg/ml would allow ingestion of approximately 1.6 mg of pefloxacin per mouse per day, or the 64-mg/kg recommended daily dose (9). Water consumption in mice receiving pefloxacin was also monitored to verify pefloxacin intake.

**Glucan therapy.** Endotoxin-free glucan was purchased from Tulane University School of Medicine (New Orleans, La.). This glucan preparation was a soluble (1-3)-beta-D-glucan isolated from the inner cell wall of *Saccharomyces cerevisiae* (4). Glucan was intravenously administered 1 h after irradiation at a dose of 5 mg per mouse. This dose has previously been demonstrated to be an effective hemopoietic stimulant in irradiated C3H/HeN mice (25). Control mice were injected intravenously with saline.

**Survival assays.** Mice entered into survival studies were irradiated with 7.9 Gy of  $^{60}\text{Co}$ . In preliminary studies, this radiation dose was determined to be lethal for approximately 80% of tap-water-maintained mice within 30 days postexpo-

sure. Survival of irradiated mice was checked and recorded daily for 30 days; on day 31, surviving mice were euthanized by cervical dislocation. Each treatment group consisted of 10 to 20 mice; experiments were repeated three to five times.

**Hemopoietic assays.** The endogenous spleen CFU (E-CFU) assay (34) was used in initial studies to screen for pefloxacin-induced inhibition of hemopoiesis. Mice were exposed to 6 Gy of  $^{60}\text{Co}$  radiation to partially ablate endogenous hemopoietic stem cells yet ensure the survival of all mice for at least the 12 days required for E-CFU detection. On day 12 postirradiation, mice were euthanized by cervical dislocation and the spleens were removed. Spleens were fixed in Bouin's solution, and grossly visible spleen colonies, arising from the clonal proliferation of surviving endogenous multipotent hemopoietic stem cells, were counted. Each treatment group consisted of five mice. Experiments were repeated three times.

In additional studies, the effects of pefloxacin on regeneration of hemopoietic progenitor cells committed to GM-CFC development were assayed by a previously described agar GM-CFC assay (23). Mouse endotoxin serum (5%, vol/vol) was added to feeder layers as a source of colony-stimulating factors. Colonies (>50 cells) were counted after 10 days of incubation in a  $37^\circ\text{C}$  humidified environment containing 5%  $\text{CO}_2$ . The cell suspensions used for these assays consisted of tissues from three normal, irradiated, or treated and irradiated mice at each time point. Femurs and spleens, both major hemopoietic organs in mice, were removed from mice euthanized by cervical dislocation. Cells were flushed from femurs with 3 ml of McCoy's 5A medium (Flow Laboratories, McLean, Va.) containing 10% heat-inactivated fetal bovine serum (HyClone, Logan, Utah). Spleens were pressed through a stainless-steel mesh screen, and the cells were washed from the screen with 6 ml of medium. The numbers of nucleated cells in the suspensions were determined with a Coulter counter. Triplicate samples were plated for each cell suspension in each experiment, and experiments were repeated three times.

**Microbiological assays.** Mice were exposed to 7.9 Gy of  $^{60}\text{Co}$ , and five mice from each treatment group were randomly selected for microbiological evaluation on days 11, 13, 15, 19, and 22 after irradiation. Animals were euthanized by cervical dislocation, and the entire liver of each mouse was excised aseptically and weighed to the nearest milligram. Organs were then added to a volume of sterile 0.9% NaCl solution equivalent to 1.0 ml/100 mg of tissue and homogenized in ground-glass homogenizers (Bellco, Vineland, N.J.) at a moderate speed. The homogenates were then inoculated onto media supportive for the growth of facultative and aerobic bacteria by using sheep blood, tryptic soy, and MacConkey agars. The number of bacterial CFU per gram of liver was calculated from the number of colonies that grew on each medium. Aerobic plates were incubated at  $35^\circ\text{C}$  in air containing 5%  $\text{CO}_2$  and were observed after 24 and 48 h. Isolates were identified by standard criteria (16, 33).

**Statistics.** With the exception of survival data, all results are presented as the mean  $\pm$  1 standard error of the mean. Survival data were analyzed by the generalized Savage (Mantel-Cox) procedure (15). All other data, unless noted otherwise, were compared by the Newman-Keul's multiple comparison test following a significant one-way analysis of variance. In cases when variances among treatment groups were not uniform, comparisons were made by a Behrens-Fischer *t* test with *P* values Bonferroni corrected (32). All multiple-comparison tests were run at the 5% level.

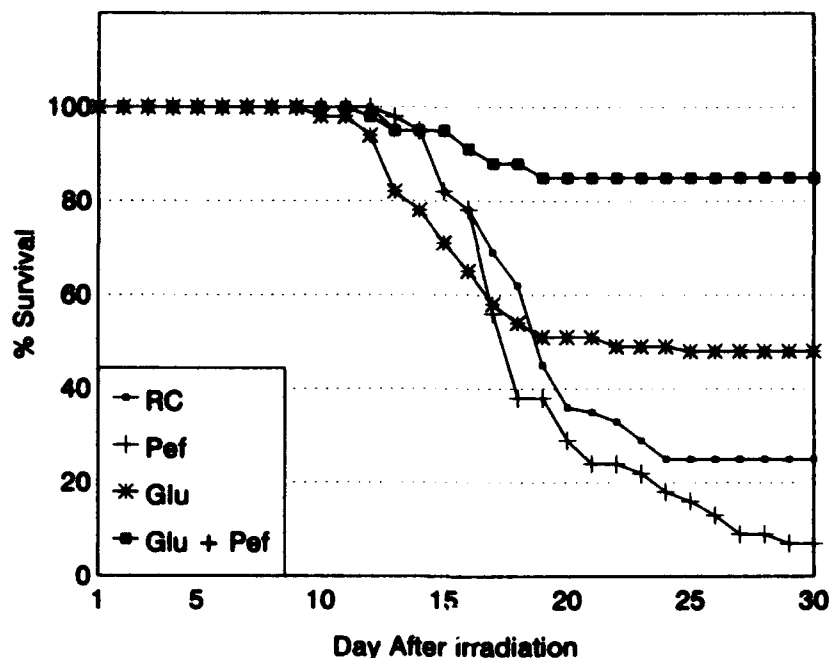


FIG. 1. Effects of pefloxacin (Pef), glucan (Glu), and glucan-pefloxacin treatments on survival of irradiated C3H/HeN mice. Mice were exposed to 7.9 Gy of  $^{60}\text{Co}$  and administered either pefloxacin (0.6 mg/ml in drinking water on days 3 to 24 after irradiation), glucan (5 mg per mouse intravenously 1 h after irradiation), or both treatments. Survival was monitored daily for 30 days. Data are a composite from five experiments, totaling 65 mice per treatment group. RC, radiation control mice.

## RESULTS

**Survival studies.** Mortality-enhancing effects of pefloxacin were consistently observed in irradiated C3H/HeN mice. On the basis of three experiments, the average 30-day survival in mice exposed to 7.9 Gy of  $^{60}\text{Co}$  and treated with pefloxacin was  $5.7\% \pm 2.9\%$ , compared with  $25.7\% \pm 3.0\%$  in radiation control mice ( $P < 0.05$ ;  $n = 45$  in each treatment group).

The ability of glucan therapy to override the mortality-enhancing effects of pefloxacin therapy in irradiated mice is illustrated in Fig. 1. This figure represents composite data from five experiments totaling 65 mice per treatment group. In contrast to the reduced survival produced by pefloxacin therapy alone (5 versus 25%;  $P < 0.05$ ), glucan therapy alone enhanced survival compared with that in radiation controls (48 versus 25%;  $P < 0.05$ ). Most interesting, however, was the ability of glucan-pefloxacin treatment to enhance survival beyond that observed with glucan therapy alone ( $P < 0.05$ ); survival in combination-treated mice was 85%. These phenomena were consistently observed in each of the five experiments performed.

We initially suspected that if the antibiotic-containing tap water produced a taste aversion, dehydration may adversely affect survival in pefloxacin-treated mice. Figure 2 illustrates that the average daily water consumption in pefloxacin-treated mice was significantly less than that of radiation control mice. However, combination-treated mice, which exhibited enhanced survival rather than impaired survival, also consumed significantly less water than radiation controls, indicating that changes in water consumption could not be correlated with survival effects.

**Hemopoietic stem and progenitor cell studies.** In the E-CFU assay, multipotent stem cells which survive the myelosuppressive 6-Gy dose of radiation should seed the spleen and

clonally proliferate to form grossly visible spleen colonies by day 12 after irradiation. When this assay was used to examine pefloxacin for the ability to inhibit hemopoietic regeneration in myelosuppressed mice, a dose-dependent reduction in E-CFU numbers was observed (Fig. 3). The E-CFU assay required that animals be euthanized on day 12 after irradiation to count the spleen colonies. For this reason, mice in these experiments were exposed to pefloxacin for only 10 days (days 3 to 12) instead of the 22-day pefloxacin treatment used in survival studies (days 3 to 24). Even following this relatively short 10-day course of pefloxacin, only  $10.4 \pm 0.5$ ,  $9.1 \pm 0.3$ , and  $5.7 \pm 0.6$  colonies were observed in mice treated with 32, 64, and 320 mg of pefloxacin per kg per day, respectively, compared with  $12.2 \pm 0.4$  colonies in radiation control mice.

Because the dose-response studies demonstrated the ability of pefloxacin to suppress hemopoiesis, the involvement of this phenomenon in enhancing mortality in irradiated mice was further evaluated. As in survival studies, mice were exposed to 7.9 Gy of  $^{60}\text{Co}$  and provided pefloxacin in the drinking water. On days 11, 13, 15, and 19 following irradiation, evaluations were performed to determine the numbers of GM-CFC progenitors in the bone marrow and spleen. In the same experiments, glucan-treated mice that also received pefloxacin were evaluated to determine whether pefloxacin-induced hemopoietic suppression could be overridden by the use of a known hemopoietic stimulant. Figure 4 illustrates the results of these studies. Compared with those in radiation control mice, both bone marrow and splenic GM-CFC recoveries were found to be suppressed in pefloxacin-treated mice. Bone marrow GM-CFC values in pefloxacin-treated mice on days 13, 15, and 19 after irradiation, respectively, were only 60, 46, and 26% of radiation control values. These data suggest that GM-CFC suppres-

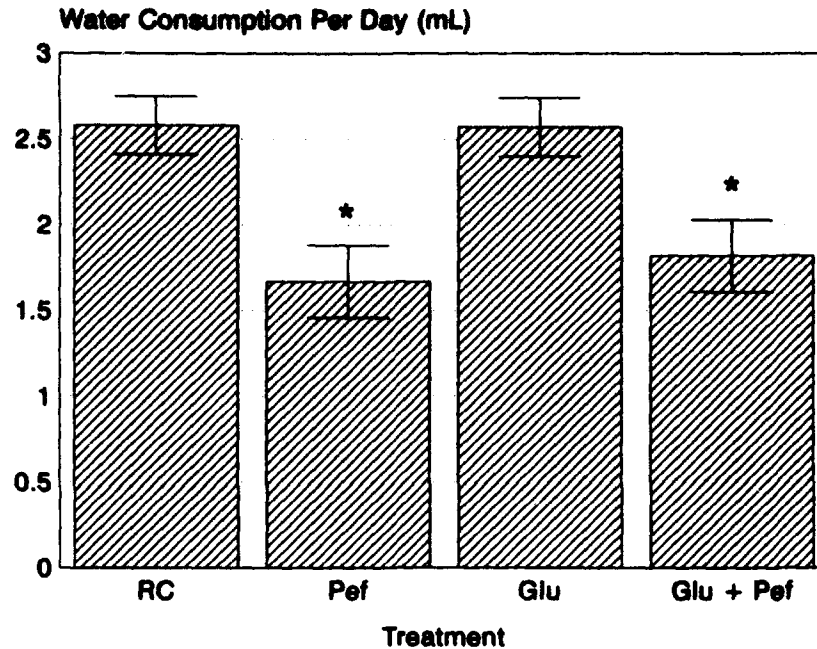


FIG. 2. Effects of pefloxacin (Pef), glucon (Glu), and glucon-pefloxacin treatments on water consumption in irradiated C3H/HeN mice. Mice were exposed to 7.9 Gy of  $^{60}\text{Co}$  and administered either pefloxacin, glucon, or both treatments as described in the legend to Fig. 1. Water consumption was measured daily through day 24 of the experiment. RC, radiation control mice; \*,  $P < 0.05$ , with respect to radiation control values or glucon values. Average daily water consumption in nonirradiated mice was  $2.8 \pm 0.6$  ml.

sion increases with the duration of pefloxacin treatment. In the spleen, GM-CFC recovery was not detected until day 19 in radiation controls ( $11.6 \pm 2.6$  GM-CFC per spleen); however, no splenic GM-CFC recovery was detected at any

time in pefloxacin-treated mice. In contrast to mice treated with pefloxacin alone, mice treated with glucon alone or glucon plus pefloxacin exhibited greater bone marrow and splenic GM-CFC recovery than did radiation control mice.

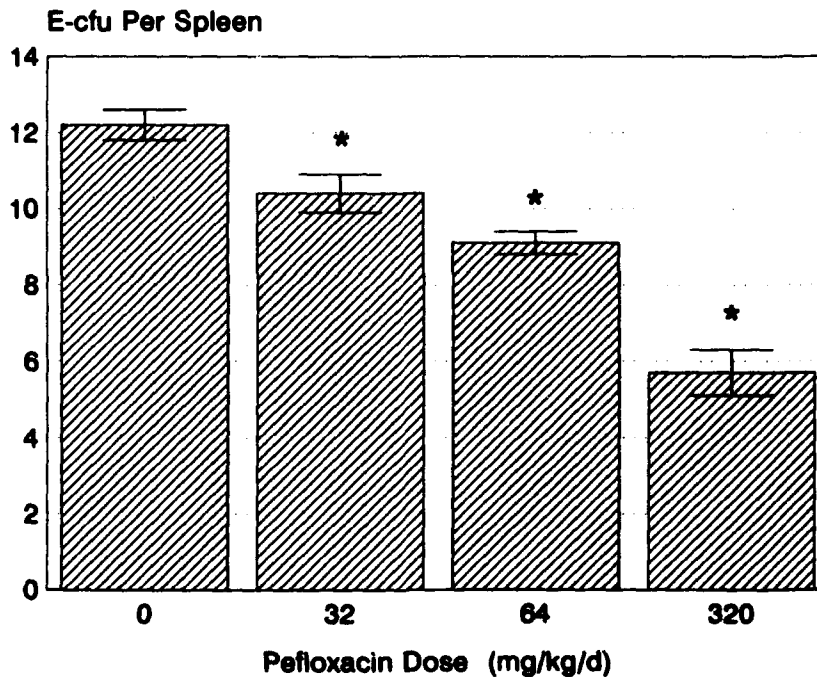
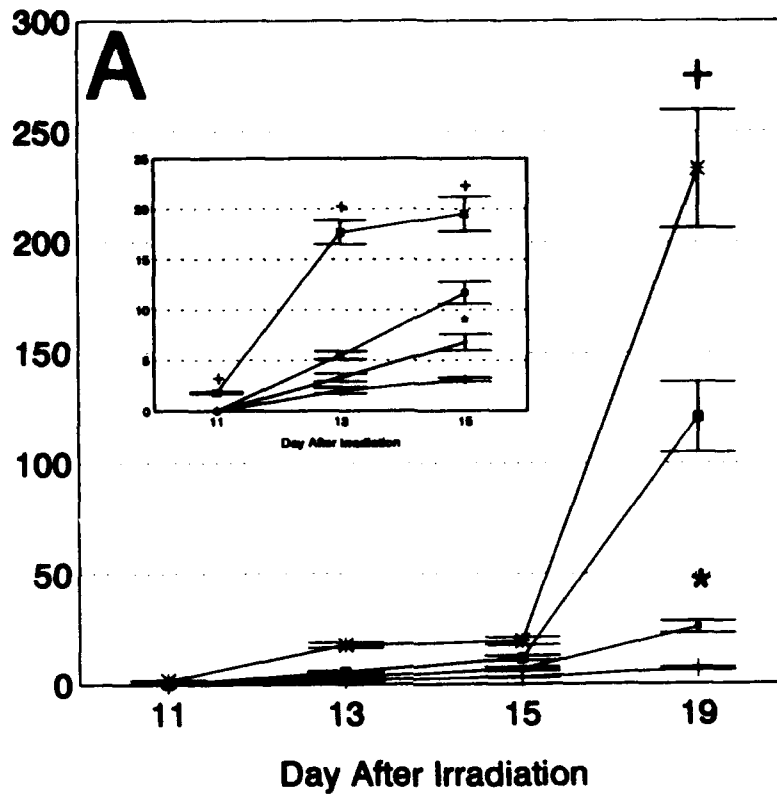
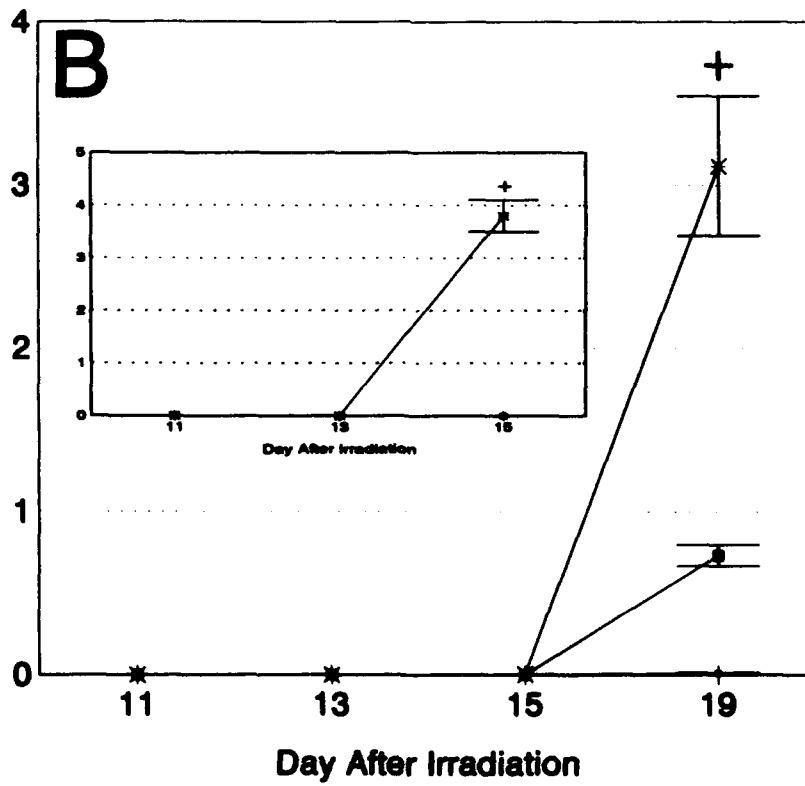


FIG. 3. Effect of pefloxacin treatment on E-CFU formation in C3H/HeN mice. Mice were exposed to 6 Gy of  $^{60}\text{Co}$  and on days 3 to 12 after irradiation were administered pefloxacin by oral gavage. Data are a composite from three experiments, totaling 15 spleens per treatment group. \*,  $P < 0.05$ , with respect to radiation control values (0 mg/kg/day) based on Dunnett's test.

GM-CFC per Femur



GM-CFC Per Spleen (Thousands)



However, recovery in glucan-pefloxacin-treated mice was less than that in mice treated with glucan only, indicating an ability of pefloxacin to dampen glucan-induced GM-CFC recovery. For example, on day 19 after irradiation, bone marrow and splenic GM-CFC recoveries in glucan-pefloxacin-treated mice, respectively, were only 52 and 24% of recoveries observed in mice treated with glucan only.

**Microbiological studies.** A *Streptococcus* sp., *Lactobacillus* spp., and occasional members of the *Enterobacteriaceae* were the predominant microorganisms recovered from the livers of mice at all time points after irradiation. The presence of these organisms may represent bacterial translocation that could lead to sepsis. Total numbers of organisms in individual mice varied greatly, and bacteria were not detected in all specimens. On days 11 and 13 after irradiation, the total number of microorganisms per gram of liver in mice treated with glucan, pefloxacin, or glucan plus pefloxacin ( $\log_{10}$  0.10 to  $\log_{10}$  0.60) was less than the total number of organisms per gram of liver in radiation control mice ( $\log_{10}$  1.61 to  $\log_{10}$  2.16). In all mice, the total number of organisms per gram of liver increased from day 15 through day 19 after irradiation and then decreased on day 22. However, on day 22 after irradiation, the total number of organisms per gram of liver in glucan-treated and glucan-pefloxacin-treated mice ( $\log_{10}$  0.10 to  $\log_{10}$  0.11) was lower than in radiation control mice or mice treated with pefloxacin only ( $\log_{10}$  0.69 to  $\log_{10}$  2.32). Interestingly, no members of the *Enterobacteriaceae* were found in mice that received pefloxacin treatment. Fungi were not detected.

#### DISCUSSION

This study demonstrates that pefloxacin therapy enhances mortality following exposure of C3H/HeN mice to midlethal radiation doses. The deleterious effect of this drug appears to be due to an inhibition of hemopoietic progenitor cell proliferation, which could be corrected through the administration of the hemopoietic stimulant glucan. Although pefloxacin appeared to reduce the number of gastrointestinal members of the *Enterobacteriaceae* that translocated through the bloodstream to the liver, the overall effect of this antimicrobial action alone was not beneficial in continually myelosuppressed mice. It may be that the eradication of gram-negative bacteria by pefloxacin reduced the normal continuous release of endotoxin into the circulation. Endotoxin in small amounts induces macrophages to produce interleukin-1 and other cytokines, including hemopoietic growth factors, that lead to increased hemopoiesis. The decreased hemopoiesis observed following pefloxacin treatment could therefore be caused indirectly by its antibacterial activity that eliminates the slow release of endotoxin. The exact cause of the mortality in mice treated with pefloxacin could not be elucidated, but suppression of hemopoietic progenitor cells would ultimately inhibit the generation of cells essential in the clearance of not only invading organisms but also cellular debris from the body. Furthermore, renal failure or electrolyte imbalance cannot be excluded as possible complications leading to mortality.

It is interesting to note that although greatest hemopoietic recovery was observed in mice treated with glucan alone, combination-treated mice exhibited the best survival. It may be that glucan in combination with pefloxacin was able to override the pefloxacin-induced hemopoietic suppression just enough to allow the production of a small but critical number of cells necessary for survival after irradiation. Because glucan also activates endogenous macrophage populations, which tend to be fairly radioresistant (30) and hence survive radiation exposures such as that used in our studies, it may also be that in combination-treated mice pefloxacin reduced the bacterial load while glucan-activated macrophages assisted in controlling the residual bacterial burden and scavenging debris even prior to the generation of new leukocytes.

In contrast to the results of this study performed with C3H/HeN mice, a previous study demonstrated the ability of pefloxacin to enhance survival in irradiated B6D2F1 mice (2). Because C3H/HeN mice contain fewer stem and progenitor cells than B6D2F1 mice (21, 28), following any given radiation dose, these cells will be reduced to a more critical level in C3H/HeN mice than in B6D2F1 mice. Therefore, it is tempting to attribute the detrimental effects of pefloxacin on survival in C3H/HeN mice to a radiation-induced reduction in stem and/or progenitor cell numbers to such a critical level that coupled with reduced regeneration, survival is further impaired. For example, the gamma radiation dose that reduces murine femoral GM-CFC numbers to 37% ( $D_{01}$ ) within 24 h after exposure is approximately 1.4 Gy (17, 26). Since B6D2F1 mice contain approximately 11,500 GM-CFC per femur while C3H/HeN mice contain only about 3,500 per femur, a 1.4-Gy radiation dose would theoretically decrease femoral GM-CFC numbers in B6D2F1 mice to 4,255 and those in C3H/HeN mice to 1,295. Following the 7.9-Gy radiation dose used in the studies presented in this paper, only about 15 GM-CFC per femur would be expected to survive the radiation exposure. Even a slight inhibition of the proliferative potential of these few progenitor cells may produce a survival disadvantage. The effect of pefloxacin in B6D2F1 mice after exposure to a radiation dose biologically equivalent to that used in our C3H/HeN mice in terms of hemopoietic injury may clarify this issue.

Although pefloxacin-induced hemopoietic inhibition and mortality were demonstrated in our studies, it turned out that mice consumed less pefloxacin than had been anticipated; consumption of pefloxacin-treated water was about 1.75 ml/day as opposed to the anticipated 2.6 ml/day. Hence, the average pefloxacin dose per mouse was only 1.05 mg/day (about 42 mg/kg/day). Since the recommended daily pefloxacin dose is 64 mg/kg (9), even greater suppressive effects might have been observed had the recommended daily pefloxacin dose actually been consumed.

In addition to the hemopoietic inhibitory effects we observed in C3H/HeN mice, deleterious hemopoietic effects have been reported following quinolone administration to humans (11). It has been known from *in vitro* studies that quinolone antibiotics can penetrate and accumulate within

FIG. 4. Effects of pefloxacin (+), glucan (\*), and glucan-pefloxacin (■) treatments on bone marrow (A) and spleen (B) GM-CFC recovery in irradiated C3H/HeN mice. Mice were exposed to 7.9 Gy of  $^{60}\text{Co}$  and administered either pefloxacin, glucan, or both treatments as described in the legend to Fig. 1. □, radiation control mice. Insets expand GM-CFC responses observed at early time points. Above the standard error bars are indicated significant differences between radiation control and pefloxacin treatments (\*) and significant differences between glucan and glucan-pefloxacin treatments (+). Average GM-CFC values per femur and per spleen from nonirradiated mice were  $1,924 \pm 80$  and  $1,360 \pm 93$ , respectively.

mammalian cells (5). Although less toxic to mammalian cells than to bacteria, high concentrations (above 25 mg/l) of quinolones have been shown to inhibit mammalian DNA replication (7, 10, 13). Additionally, decreased production of superoxide anion by human polymorphonuclear leukocytes, decreased production of immunoglobulins by human lymphocytes, reduced lymphocyte proliferation in response to phytohemagglutinin, decreased interleukin-2 production by lymphocytes, and decreased interleukin-1 production by monocytes have been demonstrated to occur following in vitro exposures to quinolones, including pefloxacin (6, 8, 9, 29).

Since in some instances quinolones have shown promise for the prevention (2) and/or treatment (3) of bacterial sepsis in irradiated mice, their use in humans exposed to radiation is being considered (12). However, because our studies in animals demonstrate that the quinolone pefloxacin can suppress bone marrow recovery and inhibit survival following severe radiation-induced myelosuppression, caution in the use of this agent in severely myelosuppressed patients may be warranted until it is determined whether such effects can also occur in humans. Further studies are needed to explore the hemopoietic effects of other quinolones in irradiated animals and whether in addition to broad-spectrum immunomodulators such as glucan, hemopoietic growth factors such as granulocyte or granulocyte-macrophage colony-stimulating factor could be used to overcome detrimental hemopoietic effects, should they occur.

#### ACKNOWLEDGMENTS

We acknowledge the excellent technical assistance of Brian Solberg and Roxanne Fischer and the editorial assistance of Modeste Greenville.

This work was supported by the Armed Forces Radiobiology Research Institute, Defense Nuclear Agency, under work units 00129 and 00132.

#### REFERENCES

1. Benacerraf, B. 1960. Influence of irradiation on resistance to infection. *Bacteriol. Rev.* 24:35-40.
2. Brook, L., and T. B. Elliott. 1991. Quinolone therapy in the prevention of mortality after irradiation. *Radiat. Res.* 128:100-103.
3. Brook, L., T. B. Elliott, and G. D. Ledney. 1991. Quinolone therapy of *Klebsiella pneumoniae* sepsis following irradiation: comparison of pefloxacin, ciprofloxacin and ofloxacin. *Radiat. Res.* 122:215-217.
4. DiLuzio, N. R., D. L. Williams, R. B. McNamee, B. F. Edwards, and A. Kitahama. 1979. Comparative tumor-inhibitory and anti-bacterial activity of soluble and particulate glucan. *Int. J. Cancer* 24:773-779.
5. Easmon, C. S. F., and J. P. Crane. 1985. Uptake of ciprofloxacin by macrophages. *J. Clin. Pathol.* 38:442-444.
- 5a. Elliott, T. B., G. Madonna, and M. Calvert. Unpublished data.
6. Fantoni, M., E. Tamburrini, F. Pallavicini, A. Antinobi, and P. Nervo. 1988. Influence of ofloxacin and pefloxacin on human lymphocyte immunoglobulin secretion and on polymorphonuclear leukocyte superoxide anion production. *J. Antimicrob. Chemother.* 22:193-196.
7. Forsgren, A., A. Bredberg, and K. Riesbeck. 1989. New quinolones: in vitro effects as a potential source of clinical toxicity. *Rev. Infect. Dis.* 11:S1382-S1389.
8. Forsgren, A., S. F. Schlossman, and T. F. Tedder. 1987. 4-Quinolone drugs affect cell cycle progression and function of human lymphocytes in vitro. *Antimicrob. Agents Chemother.* 31:768-773.
9. Gonzalez, J. P., and J. M. Henwood. 1989. Pefloxacin: a review of its antimicrobial activity, pharmacokinetic properties, and therapeutic use. *Drugs* 37:628-668.
10. Goetz, T. D., J. F. Barrett, and J. A. Sutcliffe. 1990. Inhibitory effects of quinolone antibacterial agents on eucaryotic topoisomerases and related test systems. *Antimicrob. Agents Chemother.* 34:8-12.
11. Halkin, H. 1988. Adverse effects of the fluoroquinolones. *Rev. Infect. Dis.* 10:S258-S261.
12. Hathorn, J. W., M. Rabkin, and P. A. Pizzo. 1987. Empiric antibiotic therapy in the febrile neutropenic cancer patient: clinical efficacy and impact of monotherapy. *Antimicrob. Agents Chemother.* 31:971-977.
13. Hussey, P., G. Massa, B. Tümmler, F. Grosse, and U. Schomburg. 1986. Effect of 4-quinolones and novobiocin on calf thymus DNA polymerase  $\alpha$  complex, topoisomerases I and II, and growth of mammalian lymphoblasts. *Antimicrob. Agents Chemother.* 29:1073-1078.
- 13a. Institute of Laboratory Animal Resources. 1985. Guide for the care and use of laboratory animals. National Research Council, Washington, D.C.
14. King, A., and I. Phillips. 1980. The comparative in vitro activity of pefloxacin. *J. Antimicrob. Chemother.* 17:1-10.
15. Lee, T. E. 1980. Statistical method for survival data. Lifetime Learning Publication, Belmont, Calif.
16. Lennette, E. H., A. Balows, W. J. Hausler, and H. J. Shadowy (ed.). 1985. Manual of clinical microbiology, 4th ed. American Society for Microbiology, Washington, D.C.
17. Meijne, E. I. M., R. J. M. van der Winden-van Groenewegen, R. E. Ploemacher, O. Vos, J. A. G. David, and R. Huiskamp. 1991. The effects of X-irradiation on hemopoietic stem cell compartments in the mouse. *Exp. Hematol.* 19:617-623.
18. Montay, G., Y. Geneffon, and F. Roquet. 1984. Absorption, distribution, metabolic fate, and elimination of pefloxacin mesylate in mice, rats, dogs, monkeys, and humans. *Antimicrob. Agents Chemother.* 25:463-472.
19. Patchen, M. L., M. M. D'Alessandro, I. Brook, W. F. Blakely, and T. J. MacVittie. 1987. Glucan: mechanisms involved in its "radioprotective" effect. *J. Leukocyte Biol.* 42:95-105.
20. Patchen, M. L., M. M. D'Alessandro, M. A. Chirigos, and J. F. Weiss. 1988. Radioprotection by biological response modifiers alone and in combination with WR-2721. *Pharmacol. Ther.* 39:247-254.
21. Patchen, M. L., R. Fischer, and T. J. MacVittie. 1993. Effects of combination interleukin-6 and granulocyte colony-stimulating factor on recovery from radiation-induced hemopoietic aplasia. *Exp. Hematol.* 21:338-344.
22. Patchen, M. L., and E. Lotzova. 1981. The role of macrophages and T-lymphocytes in glucan-mediated alteration of murine hemopoiesis. *Biomedicine* 34:71-77.
23. Patchen, M. L., and T. J. MacVittie. 1985. Stimulated hemopoiesis and enhanced survival following glucan treatment in sublethally and lethally irradiated mice. *Int. J. Immunopharmacol.* 7:923-932.
24. Patchen, M. L., and T. J. MacVittie. 1986. Hemopoietic effects of intravenous soluble glucan administration. *Int. J. Immunopharmacol.* 8:407-425.
25. Patchen, M. L., T. J. MacVittie, and W. E. Jackson. 1989. Postirradiation glucan administration enhances the radioprotective effects of WR-2721. *Radiat. Res.* 117:59-69.
26. Patchen, M. L., T. J. MacVittie, B. D. Solberg, M. M. D'Alessandro, and I. Brook. 1992. Radioprotection by polysaccharides alone and in combination with aminothiols. *Adv. Space Res.* 12(2):233-248.
27. Patchen, M. L., T. J. MacVittie, and L. M. Wathen. 1984. Effect of pre- and postirradiation glucan treatment on pluripotent stem cells, granulocyte, macrophage, and erythroid progenitor cells, and on hemopoietic stromal cells. *Experientia* 40:1240-1244.
28. Patchen, M. L., T. J. MacVittie, J. L. Williams, G. N. Schwartz, and L. M. Souza. 1991. Administration of interleukin-6 stimulates multilineage hematopoiesis and accelerates recovery from radiation-induced hematopoietic depression. *Blood* 77:472-480.
29. Roche, Y., M. A. Gougerot-Pocidalo, M. Fay, D. Etienne, N. Forest, and J. J. Pocidalo. 1987. Comparative effects of quinolones on human mononuclear leukocyte functions. *J. Antimicrob. Chemother.* 19:781-790.

30. Schmidtke, J. R., and F. J. Dixon. 1972. The functional capacity of X-irradiated macrophages. *J. Immunol.* 108:1624-1630.
31. Schulz, J., P. R. Almond, J. R. Cunningham, J. G. Holt, R. Loevinger, N. Suntharalingam, K. A. Wright, R. Nath, and D. Lempert. 1983. A protocol for the determination of absorbed dose from high energy photon and electron beams. *Med. Phys.* 10:741-771.
32. Snedecor, G. W., and W. G. Cochran. 1980. *Statistical methods*, 7th ed. Iowa State University Press, Ames.
33. Sutter, V. L., D. M. Citron, A. C. Edelstein, and S. M. Finegold (ed.). 1985. *Wadsworth anaerobic bacteriology manual*, 4th ed. Star Publishing, Belmont, Calif.
34. Till, J., and E. McCulloch. 1963. Early repair process in marrow cells irradiated and proliferating in vivo. *Radiat. Res.* 18:96-105.

## DISTRIBUTION LIST

### DEPARTMENT OF DEFENSE

ARMED FORCES INSTITUTE OF PATHOLOGY  
ATTN: RADIOLOGIC PATHOLOGY DEPARTMENT

ARMED FORCES RADIOBIOLOGY RESEARCH INSTITUTE  
ATTN: PUBLICATIONS DIVISION  
ATTN: LIBRARY

ARMY/AIR FORCE JOINT MEDICAL LIBRARY  
ATTN: DASG-AAFJML

ASSISTANT TO SECRETARY OF DEFENSE  
ATTN: AE  
ATTN: HA(IA)

DEFENSE NUCLEAR AGENCY  
ATTN: TITL  
ATTN: DDIR  
ATTN: RARP  
ATTN: MID

DEFENSE TECHNICAL INFORMATION CENTER  
ATTN: DTIC-DDAC  
ATTN: DTIC-FDAC

FIELD COMMAND DEFENSE NUCLEAR AGENCY  
ATTN: FCFS

INTERSERVICE NUCLEAR WEAPONS SCHOOL  
ATTN: TCHTS/RH

LAWRENCE LIVERMORE NATIONAL LABORATORY  
ATTN: LIBRARY

UNDER SECRETARY OF DEFENSE (ACQUISITION)  
ATTN: OUSD(A)/R&AT

UNIFORMED SERVICES UNIVERSITY OF THE HEALTH SCIENCES  
ATTN: LIBRARY

### DEPARTMENT OF THE ARMY

AMEDD CENTER AND SCHOOL  
ATTN: HSMC-FCM

HARRY DIAMOND LABORATORIES  
ATTN: SLCHD-NW  
ATTN: SLCSM-SE

LETTERMAN ARMY INSTITUTE OF RESEARCH  
ATTN: SGRD-UJY-OH

SURGEON GENERAL OF THE ARMY  
ATTN: MEDDH-N

U.S. ARMY AEROMEDICAL RESEARCH LABORATORY  
ATTN: SCIENTIFIC INFORMATION CENTER

U.S. ARMY CHEMICAL RESEARCH, DEVELOPMENT, AND  
ENGINEERING CENTER  
ATTN: SMCCR-RST

U.S. ARMY INSTITUTE OF SURGICAL RESEARCH  
ATTN: DIRECTOR OF RESEARCH

U.S. ARMY MEDICAL RESEARCH INSTITUTE OF CHEMICAL  
DEFENSE  
ATTN: SGRD-UV-R

U.S. ARMY NUCLEAR AND CHEMICAL AGENCY  
ATTN: MONA-NU

U.S. ARMY RESEARCH INSTITUTE OF ENVIRONMENTAL  
MEDICINE  
ATTN: SGRD-UE-RPP

U.S. ARMY RESEARCH OFFICE  
ATTN: BIOLOGICAL SCIENCES PROGRAM

WALTER REED ARMY INSTITUTE OF RESEARCH  
ATTN: DIVISION OF EXPERIMENTAL THERAPEUTICS

### DEPARTMENT OF THE NAVY

NAVAL AEROSPACE MEDICAL RESEARCH LABORATORY  
ATTN: COMMANDING OFFICER

NAVAL MEDICAL COMMAND  
ATTN: MEDCOM-21

NAVAL MEDICAL RESEARCH AND DEVELOPMENT COMMAND  
ATTN: CODE 40C

NAVAL MEDICAL RESEARCH INSTITUTE  
ATTN: LIBRARY

NAVAL RESEARCH LABORATORY  
ATTN: LIBRARY

OFFICE OF NAVAL RESEARCH  
ATTN: BIOLOGICAL SCIENCES DIVISION

SURGEON GENERAL OF THE NAVY  
ATTN: MEDICAL RESEARCH AND DEVELOPMENT

### DEPARTMENT OF THE AIR FORCE

BOLLING AIR FORCE BASE  
ATTN: AFOSR

BROOKS AIR FORCE BASE  
ATTN: AL/OEBSC  
ATTN: USAFSAM/RZ  
ATTN: OEHL/RZ  
ATTN: AL/DEBL

OFFICE OF AEROSPACE STUDIES  
ATTN: OAS/XRS

SURGEON GENERAL OF THE AIR FORCE  
ATTN: HQ USAF/SGPT  
ATTN: HQ USAF/SGES

U.S. AIR FORCE ACADEMY  
ATTN: HQ USAFA/DFBL

### OTHER FEDERAL GOVERNMENT

ARGONNE NATIONAL LABORATORY  
ATTN: ACQUISITIONS

BROOKHAVEN NATIONAL LABORATORY  
ATTN: RESEARCH LIBRARY, REPORTS SECTION

CENTER FOR DEVICES AND RADIOLOGICAL HEALTH  
ATTN: HFZ-110

**GOVERNMENT PRINTING OFFICE**

ATTN: DEPOSITORY RECEIVING SECTION  
ATTN: CONSIGNED BRANCH

**LIBRARY OF CONGRESS**

ATTN: UNIT X

**LOS ALAMOS NATIONAL LABORATORY**

ATTN: REPORT LIBRARY/P384

**NATIONAL AERONAUTICS AND SPACE ADMINISTRATION**

ATTN: RADLAB

**NATIONAL AERONAUTICS AND SPACE ADMINISTRATION  
GODDARD SPACE FLIGHT CENTER**

ATTN: LIBRARY

**NATIONAL CANCER INSTITUTE**

ATTN: RADIATION RESEARCH PROGRAM

**NATIONAL DEFENSE UNIVERSITY**

ATTN: LIBRARY

**NATIONAL LIBRARY OF MEDICINE**

ATTN: OPI

**U.S. ATOMIC ENERGY COMMISSION**

ATTN: BETHESDA TECHNICAL LIBRARY

**U.S. DEPARTMENT OF ENERGY**

ATTN: LIBRARY

**U.S. FOOD AND DRUG ADMINISTRATION**

ATTN: WINCHESTER ENGINEERING AND  
ANALYTICAL CENTER

**U.S. NUCLEAR REGULATORY COMMISSION**

ATTN: LIBRARY

**RESEARCH AND OTHER ORGANIZATIONS**

**AUSTRALIAN DEFENCE FORCE**

ATTN: SURGEON GENERAL AUSTRALIAN DEFENCE  
FORCE

**BRITISH LIBRARY (SERIAL ACQUISITIONS)**

ATTN: DOCUMENT SUPPLY CENTRE

**CENTRE DE RECHERCHES DU SERVICE DE SANTE DES ARMEES**

ATTN: DIRECTOR

**INHALATION TOXICOLOGY RESEARCH INSTITUTE**

ATTN: LIBRARY

**INSTITUTE OF RADIOBIOLOGY, ARMED FORCES MEDICAL ACADEMY**

ATTN: DIRECTOR

**KAMAN SCIENCES CORPORATION**

ATTN: DASIAC

**NBC DEFENSE RESEARCH AND DEVELOPMENT CENTER OF THE  
FEDERAL ARMED FORCES**

ATTN: WWDBW ABC-SCHUTZ

**NCTR-ASSOCIATED UNIVERSITIES**

ATTN: EXECUTIVE DIRECTOR

**PHENIX SERVICES CORPORATION**

**RUTGERS UNIVERSITY**

ATTN: LIBRARY OF SCIENCE AND MEDICINE

**UNIVERSITY OF CALIFORNIA**

ATTN: LABORATORY FOR ENERGY-RELATED HEALTH  
RESEARCH  
ATTN: LAWRENCE BERKELEY LABORATORY

**UNIVERSITY OF CINCINNATI**

ATTN: UNIVERSITY HOSPITAL, RADIOISOTOPE  
LABORATORY

**XAVIER UNIVERSITY OF LOUISIANA**

ATTN: COLLEGE OF PHARMACY